Analysis of Summer Ozone Concentrations in the Salt Lake Valley

by

Ansley Long

A thesis submitted to the faculty of
The University of Utah
in partial fulfillment of the requirements for the degree of

Master of Science

Department of Atmospheric Sciences

The University of Utah

May 2016

The University of Utah Graduate School

STATEMENT OF THESIS APPROVAL

The thesis of _____ **Ansley Long** _____

has been approved by the following supervisory committee members:

_____ **John H. Horel** _____ , Chair _____

Date Approved

_____ **Jim Steenburgh** _____ , Member _____

Date Approved

_____ **Courtenay Strong** _____ , Member _____

Date Approved

, Chair/Dean

and by _____ **Kevin D. Perry** _____ of

the

Department/College/School of _____ **Atmospheric Sciences** _____

and by David B. Kieda, Dean of The Graduate School.

ABSTRACT

Observations and analyses of ozone concentrations and near-surface wind are examined during the latter half of June 2015 when the highest ozone levels of the 2015 summer were observed in the urban areas of northern Utah referred to locally as the Wasatch Front. A novel mix of ozone observations from sensors at fixed sites as well as mobile platforms (vehicles, light rail car, and news helicopter) help to define the spatiotemporal distribution of ozone along the Wasatch Front and the nearby Great Salt Lake. The ozone and wind observations are assimilated separately using a two-dimensional variational analysis system to obtain ozone and 10 m wind analyses at 1 km horizontal resolution every hour to determine the best representation of ozone distribution throughout the region.

Two case studies are used to illustrate the diurnal evolution and transportation of ozone concentrations relative to local wind circulations driven primarily by lake-land and mountain-valley thermal contrasts. Ozone pollution roses at the fixed sensor locations for day and night periods and composites of the 1 km resolution analyses during the fifteen-day period as a function of time of day help to define common diurnal patterns. This study provides information on how ozone is distributed throughout the region and

indicates that areas of high ozone concentrations are a function of the complex

interaction of thermal flows in urban, rural, and lake boundary layers.

TABLE OF CONTENTS

LIST OF FIGURES

LIST OF TABLES

ACKNOWLEDGEMENTS

I would first like to thank my family for supporting me through this process. Without their encouragement, I would have never believed in myself enough to finish graduate school. Thanks for your endless love and support, regardless of what path I chose. There are no words to express how I feel about my friends that I have made over the last two years. I can't name all of you because so many of you have been there to help me in times of need. Thank you for supporting me the entire time. I would like to thank Utah's Division of Air Quality for funding this project. The success of GSLS03S would have not been possible without their support and cooperation. Throughout this process they have been engaged in the research conducted by our group. Their enthusiasm for understanding processes that affect local air quality is motivating and inspiring for a researcher. Lastly I would like to thank many of my professors. All of you have molded me into the graduate student I am today, both in and out of the classroom. My advisor, John Horel has exceeded all of my expectations and beyond for an advisor. I have learned so much from him and I will forever cherish and use that knowledge forever. I would also like to thank John for giving me this opportunity, as well as advocating for me. There were

some rough times but John always had my back, even if it meant going out of

his way.

CHAPTER 1

INTRODUCTION

As a result of regulations limiting ozone precursor emissions (e.g., nitrogen oxides. NO_x, and volatile organic compounds, VOC's), near-surface ozone concentrations in the United States have improved during the past 15 years (Ryerson et al. 2013; Simon et al. 2014). However, Madronich et al. (2015) discuss the health effects of ozone exposure particularly for groups that are sensitive to poor air quality (e.g., children, the elderly, and those with asthma and other respiratory illnesses). Long-term exposure to high levels of ozone contributes to lung damage that can lead to a range of illnesses, including acute and chronic bronchitis and asthma (Chen et al. 2007). As a result of the health impacts of exposure to high concentrations of ozone, the Environmental Protection Agency (EPA) lowered the National Ambient Air Quality Standard (NAAQS) from an 8-hr average ozone concentration of 75 ppb to 70 ppb (EPA 2015).

During the day, ozone is formed through photochemical reactions with the hydroxyl radical that oxidizes VOC's (Finlayson-Pitts and Pitts 1993). This

reaction yields peroxy radicals that serve as catalysts for NO_2 and ozone production in the following chain of chemical reactions:

$$OH + VOC(+ O_2) \rightarrow RO_2$$

$$RO_2 + NO \rightarrow RO + NO_2$$

$$NO_2 + hv \rightarrow NO + O$$

$$O + O_2 \rightarrow O_3$$
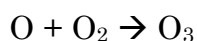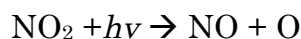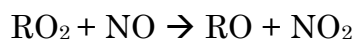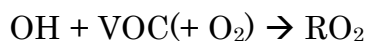
Background values of ozone are typically higher aloft in metropolitan areas particularly at night as a result of surface ozone titration (Zhang et al. 2004):

$$NO + O_3 \rightarrow NO_2 + O_2$$

The rate of titration as a result of this reaction is normally overwhelmed during the day by the photolysis of NO_2.

High ozone concentrations have been an issue for decades in the western United States with the first air pollution control district in the west created in Los Angeles County in 1947 (SCAQMD 1997). Numerous field campaigns have been undertaken to study summer ozone concentrations throughout the western states, for example in California during 1997, 2000, and 2010 (Croes and Fujita 2003; Ryerson et al. 2013). Of particular relevance to the study presented here are the previous studies examining downwind transport from urban centers and boundary-layer thermally-driven flows that modulate pollutant concentrations. Downwind transport of ozone from urban areas has been extensively studied over the years (Zeller et al. 1977; Ainslie and Stein 2005; Whaley et al. 2015; Zhang et al. 2014). The effects of sea and lake breeze

circulations on pollutant concentrations have also been examined around the world (Dye et al. 1995; Fast and Heilman 2003; Levy et al. 2010; Lin et al. 2010; Cleary et al. 2015). Through a variety of processes, ozone reservoirs may form over large bodies of water near urban areas. For example, Lin et al. (2010) found that pollutants remain over the water along Taiwan's coast at night enhancing ozone concentrations the following day. Lasry et al. (2005) found that sea breezes can transport ozone and precursors back towards urban areas and increase the rate of local ozone production. In addition, vertical lofting of ozone and its precursors as a result of lake and land breezes may contribute later to downward recirculation that allows ozone to continue to accumulate over time (Lyons and Olsson 1973; Harris and Kotamarthi 2005).

Thermally driven slope and valley flows often lead to large spatial and temporal variations in ozone concentrations (Doran and Zhong 2000; Ainslie and Stein 2007; Gheusi et al. 2011; Blaylock 2016). For example, Ghuesi et al. (2011) observed quasi-horizontal layers of varying ozone concentrations over the Pyrenees that resulted in sharp ozone gradients vertically as well as horizontally.

The Utah Division of Air Quality (DAQ) has monitored for many years high summer ozone concentrations in the metropolitan region stretching from north to south to the west of the Wasatch Mountains that is referred to locally as the Wasatch Front (Fig. 1.1). The synoptic weather conditions associated

with episodes of elevated ozone concentrations in the western United States are well established (Agel et al. 2011; Crosman and Horel 2016): large-scale ridging leading to subsidence aloft and generally clear skies. Due to its elevation of 1300-1500 m, the Wasatch Front also experiences enhanced photolysis and ozone production during high insolation periods. Arens and Harper (2012) led a field study in 2012 to examine ozone concentrations throughout northern Utah both along the metropolitan Wasatch Front as well as in nearby mountain basins and over the Great Salt Lake (GSL). They found that higher elevation mountain valley sites downwind of the Wasatch Front had similar or greater ozone concentrations than observed along the Wasatch Front. They also found that ozone concentrations along the shores of the GSL exceeded the 75 ppb NAAQS on 12 days during the 2012 summer.

Although increased regulation of emissions has helped to reduce ozone concentrations locally, the DAQ recognizes that the state of Utah faces substantive challenges to meet the current NAAQS standard for ozone during summer along the Wasatch Front. To follow upon the Arens and Harper (2013) study and improve understanding for the causes of high ozone episodes, the DAQ supported a modest field campaign during the 2015 summer, referred to as the Great Salt Lake Summer Ozone study (GSLSO$_3$S, Horel et al. 2016). The objectives of that field campaign were to: (1) determine the areal and vertical extent of ozone concentrations over and surrounding the GSL during the summer and (2) improve understanding of the meteorological processes

that control ozone formation near the GSL during summer to help DAQ forecast ozone concentrations along the Wasatch Front. DAQ forecasters indicated that predicting summer ozone concentrations was more difficult for them than forecasting winter particulate levels. Current air quality models from the National Weather Service show large concentrations of ozone over the Great Salt Lake. This study is conducted in hopes of better understanding the spatial extent of ozone makes ozone air quality forecasts more skillful.

In response to those general objectives, several studies related to the GSLSO$_3$S have been or are being completed, including this one. Horel et al. (2016) illustrated the utility of observations collected in real-time from fixed site and mobile sensors for a case during late-August 2015 when regional transport of wildfire smoke affected ozone concentrations along the Wasatch Front. Blaylock et al. (2016) contrasted the impacts of lake breezes of differing intensities on ozone concentrations in the Salt Lake Valley. They used a Weather Research Forecasting model simulation encompassing 17-18 June 2015 to examine how strong opposing flow and convergent frontogenesis at the leading edge of the lake breeze front delayed the transport of high ozone levels into the Salt Lake Valley until late afternoon on 18 June.

This study is focused on answering the following questions:

- How do local thermally-forced flows affect ozone concentrations along the Wasatch Front and in the nearby mountains?

6

- To what extent does the boundary layer over the GSL serve as a reservoir of ozone and its precursors that influences ozone concentrations along the nearby Wasatch Front?

To address these questions, observations and analyses of ozone concentrations and 10-m surface wind are examined during the latter half of June 2015 when the highest ozone levels of the summer were observed. The objective of this study is to examine more broadly the spatial and temporal evolution of ozone concentrations during this entire period than has been done in the other studies completed to date. Since the observing assets were most abundant during the GSLSO$_3$S in the southeast quadrant of Fig. 1.1, that sector of the Wasatch Front from Ogden in the north to the Salt Lake Valley to the south is emphasized. This sector also includes the Oquirrh Mountains and Tooele to the west and Wasatch Mountains to the east. For further reference, the main southern stem of the GSL is referred to as Gilbert Bay, while the nearly dessicated eastern branch of the GSL is called Farmington Bay.

As a means to visualize the spatial and temporal differences in ozone in the aforementioned region and period, 1-km horizontal resolution analyses of ozone concentrations and surface wind at 1-hr intervals were created using the University of Utah's two-dimensional variational analysis (UU2DVAR) data assimilation system (Tyndall and Horel 2013). Case studies documenting the diurnal evolution of ozone concentrations are presented for 18 and 27 June

2015. In addition, 15-day averages (16-30 June 2015) are used to illustrate the

typical diurnal evolution of ozone concentrations and surface wind.

Figure 1.1. Region of interest for this study and areal extent of the Great Salt
Lake during summer 2015.

CHAPTER 2

DATA AND METHODS

2.1 Observational data

Horel et al. (2016) summarize the observational assets available during

GSLSO$_3$S. The GSLSO$_3$S web site (http://meso2.chpc.utah.edu/gslso3s)

provides access to archived data and other resources pertinent to this study.

As shown in Fig. 2.1a, meteorological parameters such as temperature,

moisture, and wind are available at over a hundred locations from MesoWest

(Horel et al. 2002). During the 2015 summer, federal equivalent method ozone

sensors at long-term air quality observing sites managed by the DAQ along the

Wasatch Front were supplemented by 2B Technology Model 202 ozone sensors

deployed at sixteen additional sites (Fig. 2.1b). The United States Forest

Service also maintains an ozone sensor at the Snowbird ski area in Little

Cottonwood Canyon in the Wasatch Mountains.

Mobile observations during selected periods of the summer were

available from sensors mounted on a TRAX light rail car (Fig. 2.1b) and

instrumented vehicles (Fig. 2.1c). In addition, Fig. 2.2 provides a heat map of

the observations available from the KSL news helicopter during 16-30 June 2015.

2.2. UU2DVAR analyses

The University of Utah Variational Surface Analysis (UU2DVAR) system described by Tyndall and Horel (2013) was modified to provide 1 km analyses for 2 m air temperature, 2 m dewpoint temperature, surface pressure, 10 m u and v wind components, wind speed, and ozone concentration. This univariate two-dimensional variational data assimilation technique allows for the minimization of the variational cost function, $J(x_a)$,

$$y_o - \mathrm{H}(x_b) = (\mathrm{H}\mathrm{P_b}\mathrm{H}^\mathrm{T} + \mathrm{P_o})\eta$$

(1)

where $x_a$observation (y_o) increments relative to the background grid (x_b) are mapped to the observation locations by the forward operator (H). The background ($\mathrm{P_b}$) and observation ($\mathrm{P_o}$) error covariances are defined a priori. The term η is computed by iteratively solving (1), and is used to yield the analysis $x_a$in (2) (Tyndall 2013):

$$x_a = x_b + \mathrm{P_b}\mathrm{H}^\mathrm{T}\eta$$

(2)

Table 2.1 summarizes some of the characteristics of the analyses after subjective evaluation was undertaken to estimate appropriate parameters for the observational to background error variance ratio and length scales over which background errors at grid points separated horizontally and vertically

from one another are assumed to become decorrelated (see Tyndall and Horel 2013). Meteorological 1-hr forecasts grids from the High Resolution Rapid Refresh (HRRR) model are interpolated from 3 km to 2.5 km at the National Centers for Environmental Prediction for use by the Real-Time Mesoscale Analysis. Those grids are then further interpolated to 1 km at the University of Utah for use as the background grid (x_b) for all fields except ozone concentration. The analyses are computed for this study encompass roughly the area shown in Figs. 1.1 and 2.1 bounded by 40.25- 41.75oN and 111.75-113.25oW. However, the analyses shown here are for the southeastern sector of the analysis grid where the ozone and wind observations are most abundant.

The background ozone values are generated each hour from subsets of station observations. This approach violates the assumption implicit in variational analyses that the background field and observations are independent of one another (Kalnay 2003). However, this approach can be viewed simply as a statistical optimum interpolation approach selecting a priori appropriate relative weights for the background and observations.

Some general differences in the ozone concentrations are assumed to exist between grid points in rural land locations, across the lakeshore, along the urban corridor, and in the Wasatch Mountains. Concentrations in each of those general categories are expected to vary with elevation. Arbitrarily, a rectangle was defined by the coordinates 40.3-41.3oN and 111.75-112.05oW to encompass much of the urban corridor along the Wasatch Front as well as the

Wasatch Mountains. All land grid points outside of this grid box are defined

for convenience as being rural. Linear regression each hour between elevation

and ozone concentrations at the eight rural sites listed in Table 2.2 is then used

to define the background ozone value for every rural grid point as a function of

that grid point's elevation. Background values at rural grid points above

1500 m are linearly constrained by the Farnsworth Peak (FWP) site located at

the crest of the Oquirrh Mountains to the west of the Salt Lake Valley. This

station is most representative of rural, high elevation sites throughout the

domain and also is the best estimate within the analysis domain for ozone

concentrations in the free atmosphere above the urban and rural boundary

layers.

All grid points classified as falling in the GSL are assigned the median

hourly value available from the eight lakeshore sites listed in Table 2.2.

However, the HRRR's excessively large estimate of the lake's areal extent

required that the UU2DVAR lake-land mask had to be adjusted. The summer

2015 satellite image in Fig. 1.1 was used to redraw the lake's boundary for use

in the analysis system.

Linear regression each hour between elevation and ozone concentrations

at the eleven urban sites listed in Table 2.2 is then used to define the

background ozone value for the urban grid points as a function of each grid

point's elevation. Background values at urban grid points above 1500 m are

linearly constrained by the Snowbird (S2OZN) site located in the Wasatch

Mountains to the east of the Salt Lake Valley, i.e., that site is likely most representative of the ozone concentrations in the vicinity of the Cottonwood Canyons within the Wasatch Mountains, but it is assumed here that those concentrations are representative of ozone levels in other sectors of the Wasatch Mountains as well.

The arbitrary definition of the background grids introduces occasional recognizable discontinuities in the subsequent analyses in data void regions, e.g., across the rectangle's boundary that defines the urban zone. However, the purpose of the background field is simply to provide a means to build in weak dependence on elevation in data sparse regions yet allow for the spatial differences arising from the observations themselves to dominate.

The background error covariance $(\mathbf{P_b})$ is assumed to vary horizontally and vertically and depend on horizontal (R) and vertical (Z) error decorrelation length scales:

$$\mathbf{P}_{\mathbf{b}_{ij}} = \sigma_b \exp\left(-\frac{r_{ij}^2}{R^2}\right) \exp\left(-\frac{z_{ij}^2}{Z^2}\right) \tag{3}$$

where σ_b is the background error variance and r_{ij} and z_{ij} are the horizontal and vertical distances between grid points i and j. Following Tyndall and Horel (2013), grid points over the lake are assumed to be 500 m lower to minimize the influence of observational increments at land sites from influencing those over the lake and vice versa. Then, to allow ozone observations at 5 of the lakeshore sites to largely control the analyzed ozone

values offshore, each of those lakeshore observation was bogused to a nearby lake grid point as shown in Fig. 2.2b. When available, mobile observations collected on the causeway that splits the GSL as well as those collected on the causeway out to Antelope Island were assumed to be located on lake grid points.

Table 2.1 summarizes the assumptions made regarding the observation to background error variance ratio (σ_o^2/σ_b^2) and horizontal and vertical decorrelation length scales. For the meteorological fields, the HRRR background grids are assumed to be good and observations can be of varying quality (e.g., ratios for National Weather Service sites set to 1 while for Citizen Weather Observing Program sites set to 2.5).

Because of the extensive manual quality control applied to the ozone data, we have confidence in drawing the analysis closer to the ozone observations than to the assumed background values. Hence, the ratio of fixed-site ozone observation error variance to the background error variance is set to 0.8. Ozone observations from mobile platforms are assumed to have higher errors, so the error variance ratio for them is set to 1-1.5 with higher error variance for mobile observations over 15 min from the top of the hour (up to 12 mobile observations at 5 min intervals from ±30 min relative to the top of the hour can be used in the analyses). As will be shown in the next chapter, news helicopter flights during most of the day occur when the well-mixed boundary layer is 1-2 km deep. Hence, ozone values measured aloft from the helicopter

are assumed to be similar to those observed near the surface and whenever the helicopter is within 300 m of the underlying terrain, the helicopter observations are treated as if they were at the surface.

Fig. 2.3 illustrates some of the features of typical ozone concentration analyses when all available observations are used (Fig. 2.3a) and when only fixed sites are used (Fig. 2.4b). Blaylock et al. (2016) showed that a strong lake breeze front led to a gradient in ozone concentration down the Salt Lake Valley at this time (1600 MDT 18 June 2015) with higher (lower) concentrations in its northern (southern) end. Based on the Farnsworth Peak (FWP) observation at the crest of the Oquirrhs, free atmosphere ozone concentrations lie in the 55-60 ppb range, while concentrations are 5 ppb higher at Snowbird (S2OZN) in the Wasatch Mountains. The analysis procedure then leads to similar values at other elevations of those respective ranges. When only the fixed site observations are used (Fig. 2.3b), ozone concentrations of 70-75 ppb observed at Badger Island (BGRUT) on the western edge of the GSL and along the Wasatch Front to the north of the Salt Lake Valley lead to analyzed values similar to those observed in those locales over land. (The circular 70-75 ppb shaded half-ring over the GSL to the west of BGRUT reflects the imposed bogused BGRUT observation.) Ozone levels decrease 10 ppb from north to south to the north of the Salt Lake Valley.

When all of the available observations are used (Fig. 2.3a), lower concentrations are analyzed along the northern fringe of the figure as a result

of the observation during this hour from a vehicle mounted sensor travelling along the causeway across the GSL. Mobile observations from sensors on two vehicles, a light rail car and the new helicopter overlap in the northern end of the Salt Lake Valley into Davis County to its north. The net effect of all of these mobile observations is to shift the 10 ppb gradient further south, sharpen it, and make the concentrations more uniform to the south of it. Blaylock et al. (2016) highlight that this gradient became even sharper during the next hour. The differences between the two analyses shown in Fig. 2.3c illustrate the lowered concentrations along the causeway (and the artificial shape to those changes resulting from the assumed horizontal decorrelation error length scale). The helicopter transect extending down into the Salt Lake Valley combined with the other mobile observations lead to lower ozone levels in the Salt Lake Valley as well.

As with all variational analysis systems in which the background error decorrelation length scales are assumed a priori, observations in data sparse regions will often lead to artificial geometric structures in the analyses while many observations of dissimilar values in close proximity tend to be smoothed out. Figure 2.4 illustrates the relatively weak sensitivity of the ozone analysis for 1600 MDT 18 June 2015 to changes in the vertical and horizontal decorrelation error length scales (the wind fields are identical in the panels). Reducing the length scales to 15 km horizontally and 150 m vertically (top left corner) tends to narrow the influence of observations too much, driving more

of the analysis towards the assumed background values in data limited regions. Increasing the horizontal length scale to 35 km and 350 m vertically (bottom right corner) tends to broaden their influence and smooth the analysis too much. Hence, the middle values are the ones ultimately chosen for the ozone analyses (Table 2.1).
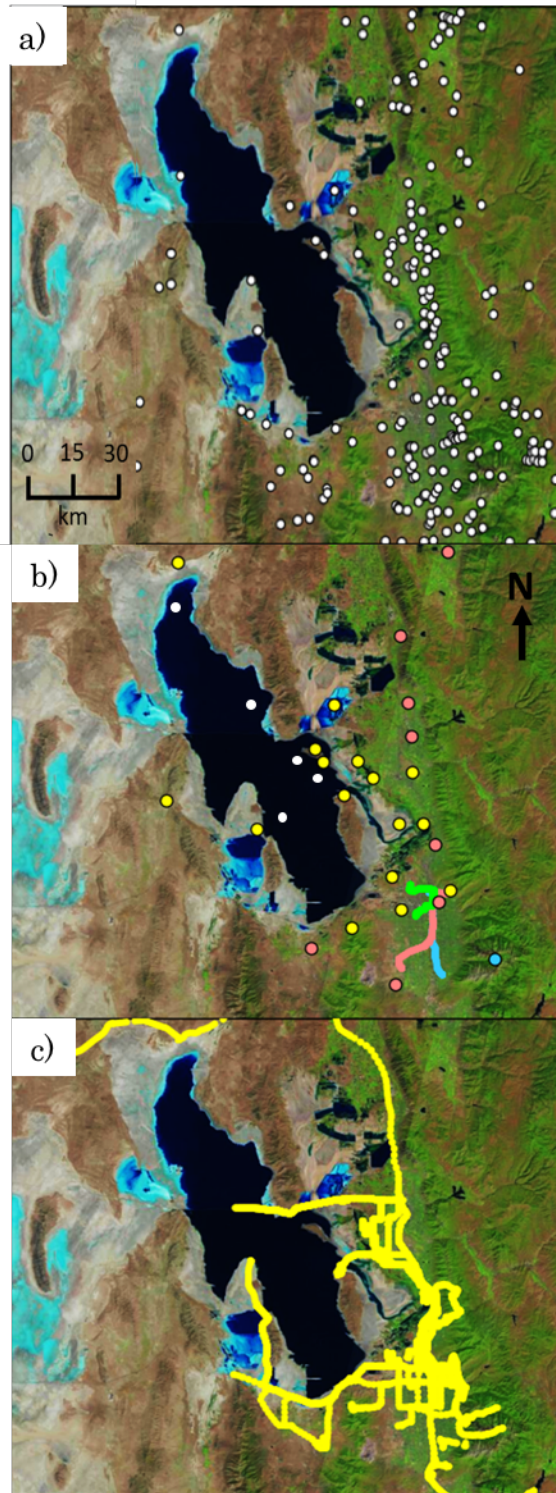
Figure 2.1. Location of selected instrumentation during the GSLSO₃S. a) meteorological monitoring locations. b) ozone monitoring at permanent DAQ (red circles) and United States Forest Service (blue circle) sites, season-long sites (yellow circles), bogus ozone sites assumed from lakeshore locations over GSL (white circles) as well as routes of the light-rail car on Red, Green, and Blue lines in the Salt Lake Valley. permanent DAQ monitoring sites. c) cumulative ozone monitoring routes of vehicles (yellow).
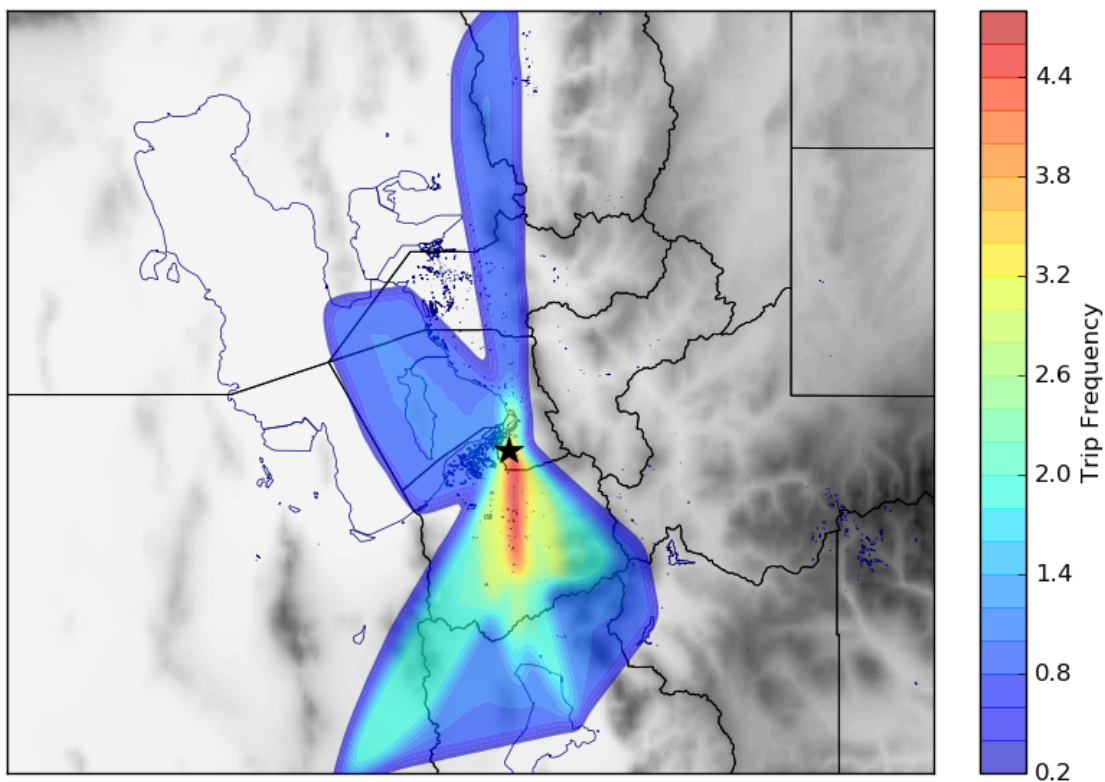

Figure 2.2. Number of flights available available from the KSL news helicopter during the 16-30 June 2015 period.
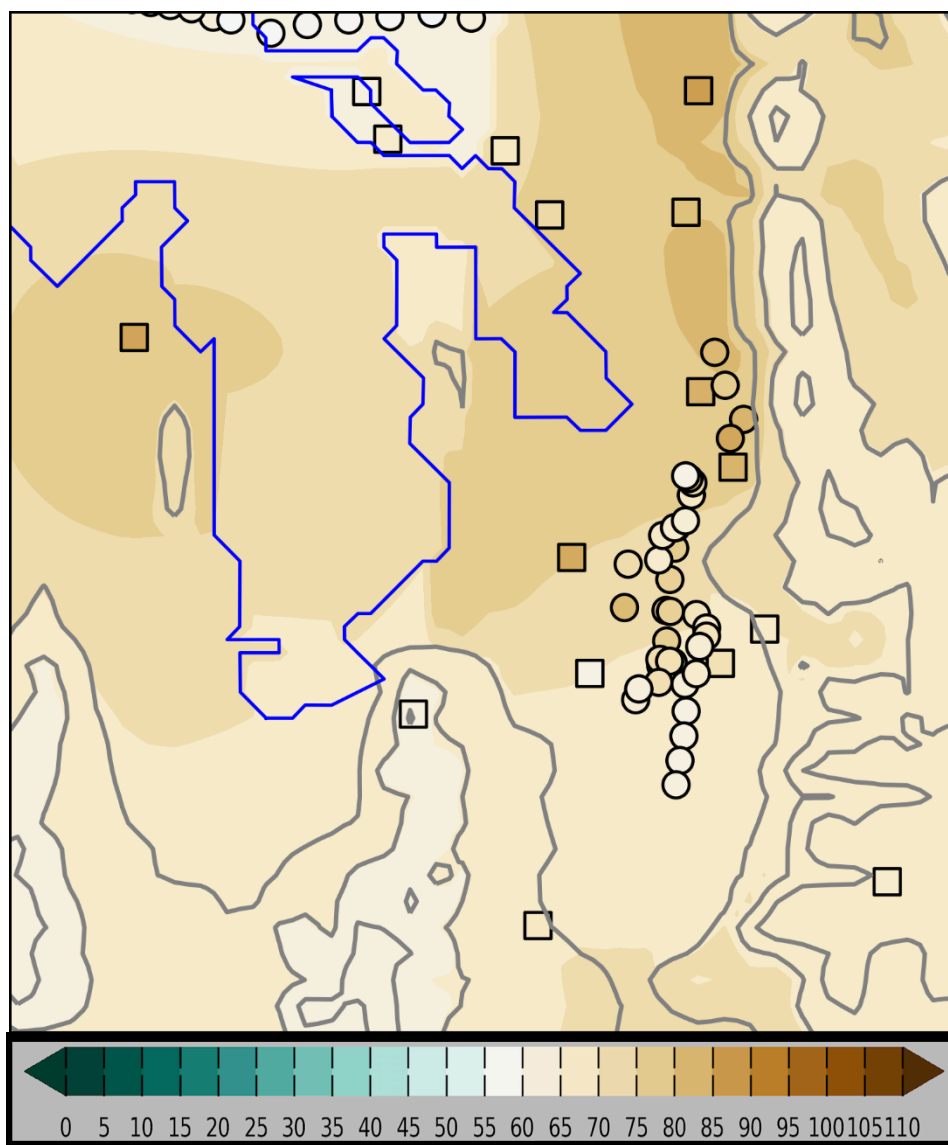
Figure 2.3.a. UU2DVAR ozone concentration analysis (in ppb with shading according to the colorbar) for 1600 MDT 18 June 2015 using all available observations. Observations from fixed sites are denoted by squares while mobile observations used in the analysis are denoted by circles. Elevation contoured in light grey at 500 m intervals beginning at 1500 m.
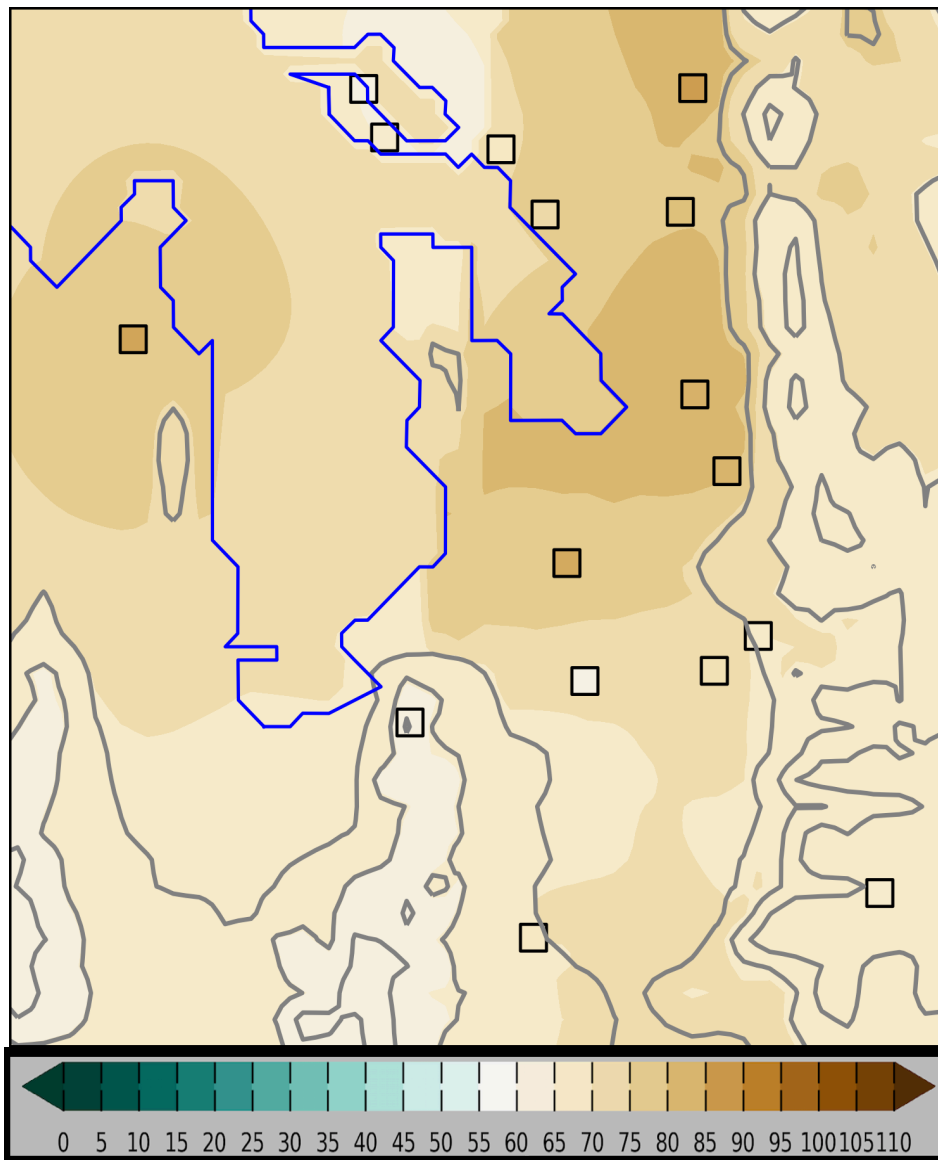
Figure 2.3.b. UU2DVAR ozone concentration analysis (in ppb with shading according to the colorbar) for 1600 MDT 18 June 2015 using observations from fixed sites (squares) only. Elevation contoured in light grey at 500 m intervals beginning at 1500 m.
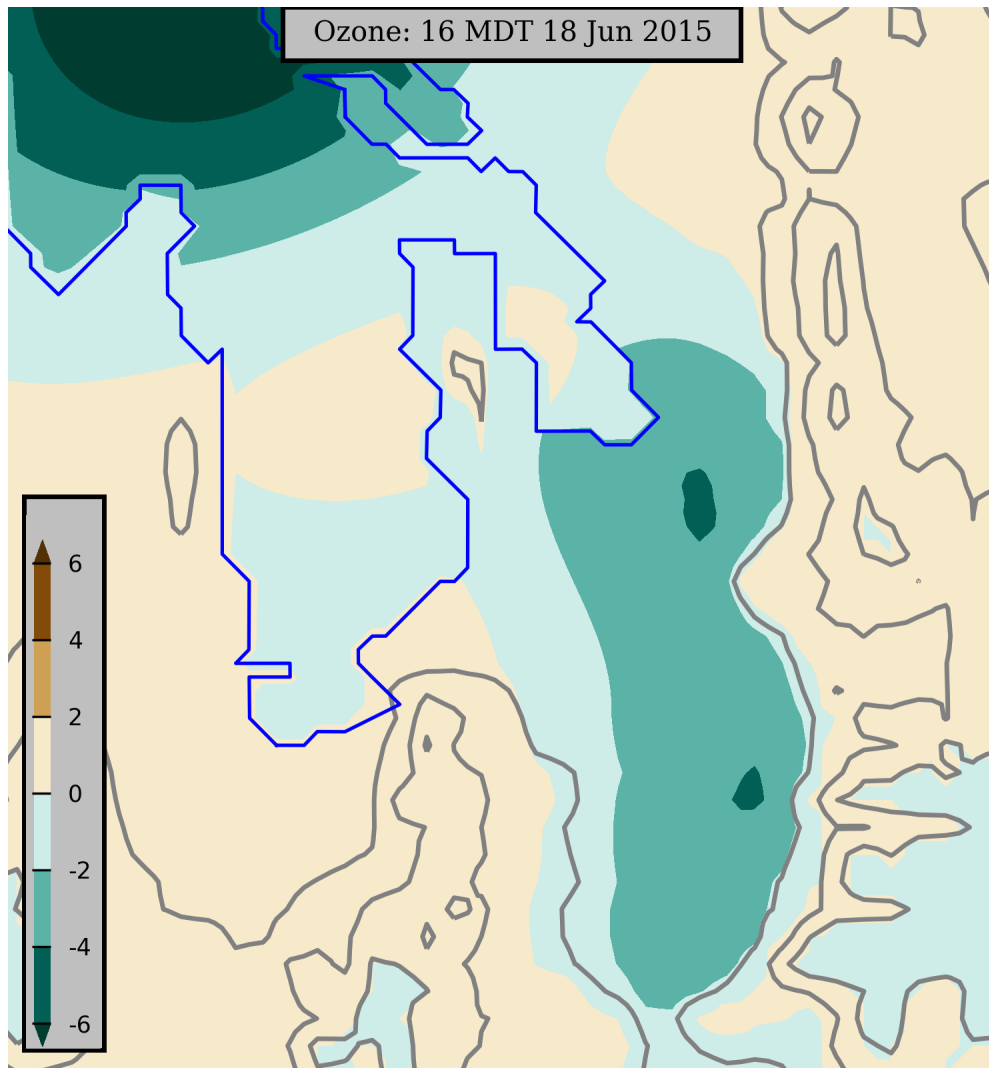
Figure 2.3.c. Ozone concentration difference (pbb) according to the colorbar between the analysis using all available observations (Fig. 2.4a) and the analysis without mobile observations (Fig. 2.4b). Elevation contoured in light grey at 500 m intervals beginning at 1500 m.
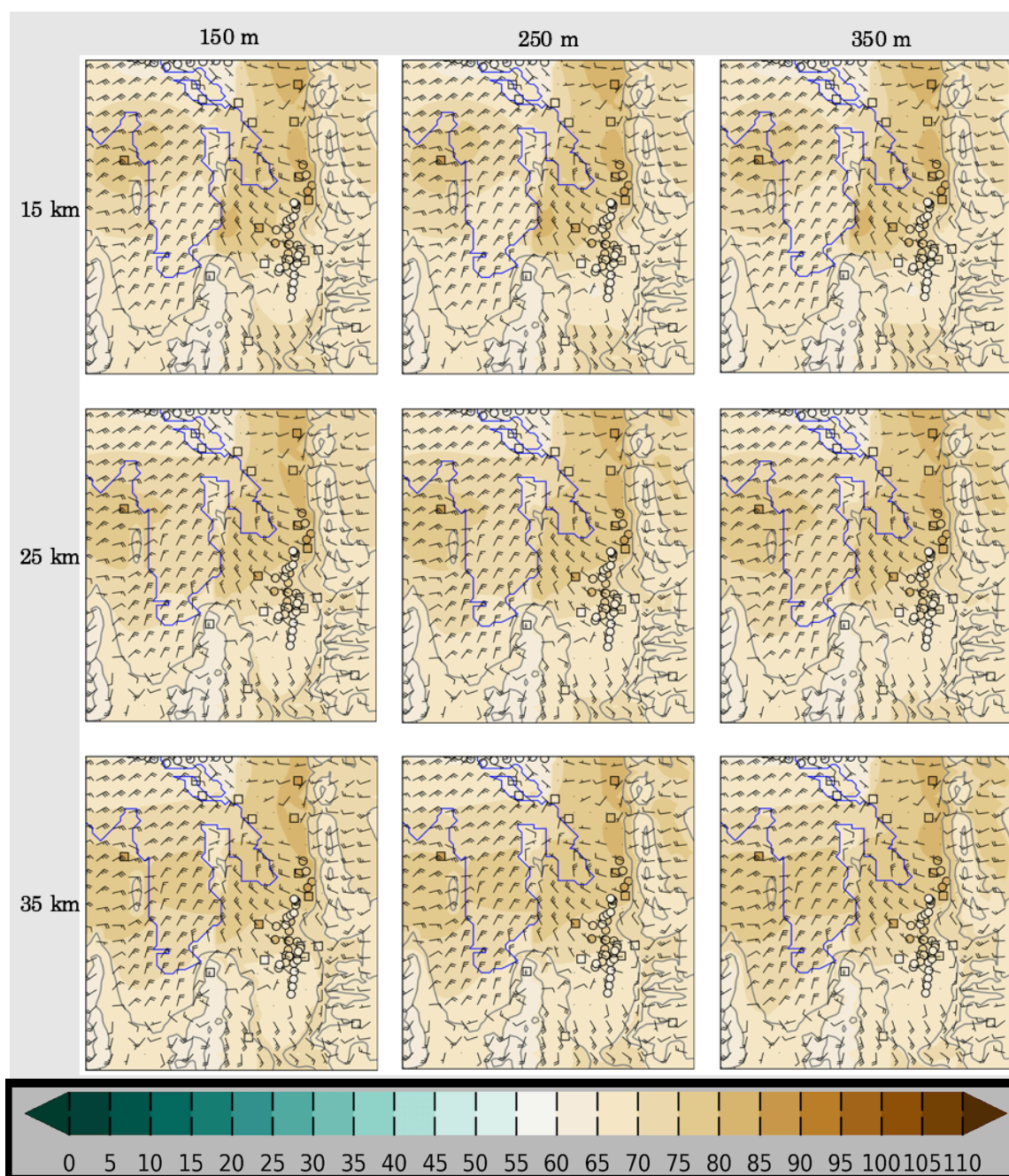
Figure 2.4. UU2DVAR sensitivity to horizontal (rows) and vertical (columns) background decorrelation length scales for 1600 MDT 18 June 2015. Ozone concentrations for the analyses and permanent (square) and mobile (circle) observations indicated by the colorbar (ppb). Elevation contoured in light grey at 500 m intervals beginning at 1500 m. Vector wind analyzed at every 4th gridpoint superimposed where half and full barbs denote speeds of 1.0 and 2.0 m s^{-1}.

Table 2.1 Summary of UU2DVAR analysis characteristics and parameters used in this study.

Type	Background	Observations to background error variance ratio	Horizontal (R) and vertical (Z) background error decorrelation length scales
Wind, temperature, moisture	HRRR interpolated to 1 km grid	1-2.5 depending on observational network type	25 km/250 m
Ozone Concentration	Statistical fits to subsets of observations	0.8 for fixed site and 1-1.5 for mobile observations	25 km/100 m

Table 2.2 Stations with associated abbreviations in the rural, lakeshore, and urban categories. Observations at lakeshore sites in red were also repeated offshore as bogus observations.

Rural (a)	Lakeshore (b)	Urban(c)
Locomotive Springs (LMS)	Badger Island (BGRUT)	Mountain Meteorology (MTMET)
Great Salt Lake Minerals (GSLM)	Locomotive Springs (LMS)	Neil Armstrong Academy (NAA)
Lakeside (O3S06)	Great Salt Lake Minerals (GSLM)	Hill Air Force Base (O3S04)
Erda (QED)	Kate's Point (O3S07)	Brigham City (QBR)
Logan (QL4)	Syracuse (QSY)	Bountiful (QBV)
Brigham City (QBR)	Ogden Bay (O3S01)	Herriman (QH3)
Farnsworth Peak (FWP)	Farmington Bay (O3S02)	North Provo (QNP)
Snowbird (S2OZN)		Ogden (QO2)
		Saltaire (QSA)
		Spanish Fork (QSF)
		Hawthorne (QHW)

CHAPTER 3

RESULTS

3.1 Ozone concentrations during 16-30 June 2015

The focus of this study is on the 16-30 June 2015 period when the highest ozone concentrations of the summer were observed in the Salt Lake Valley. Large-scale ridging aloft dominated with high temperatures, generally light winds, and mostly clear skies. In contrast to mid-August 2015 when regional transport of smoke impacted ozone concentrations (Horel et al. 2016), the production and destruction of ozone during the latter half of June appeared to be dominated by local sources and processes. The time series in Fig. 3.1a illustrates the high levels of solar radiation in the Salt Lake Valley near the summer solstice with occasional small decreases primarily during late afternoons arising from intermittent cloud cover.

The numbers of ozone measuring sites in the rural, lakeshore, and urban categories (Table 2.2) that exceed the NAAQS of 70 ppb over an 8-hr period are shown in Fig. 3.2 for each day. Of the 8 rural sites, at least one location exceeded the standard on 13 of the 15 days while at least one of the 8 GSL shore sites exceeded the standard for 11 of the 15 days. Not unexpectedly, the

large amounts of incoming solar radiation combined with abundant concentrations of precursor chemicals led to at least one of the 11 urban sites to exceed the standard during all but one of the days during this period.

Figure 3.3 shows the time series of 8-h running means of ozone concentration for sites in the rural, lakeshore, and urban categories. The diurnal cycle dominates at each site, but the amplitudes of the diurnal variations vary widely. For example, with the exception of the "rural" site in Logan (QL4, lower purple curve in Fig. 3.3a) that has a city population of ~50000, all of those sites tend to have small diurnal ranges with ozone concentrations during this period primarily between 40 and 70 ppb. Lakeshore sites far removed from the Wasatch Front urban corridor have similar small diurnal ranges while those close to the Wasatch Front tend to experience nocturnal titration dropping ozone levels to ~20 ppb while reaching peaks over 70 ppb in the afternoon (Fig. 3.3b). As expected, large diurnal swings with lower minima are observed in the Wasatch Front's urban corridor where titration prevails at night.

Horel et al. (2016) used ozone air pollution roses in the vicinity of the Salt Lake Valley to summarize the ozone concentrations as a function of wind direction during the night (8 PM – 8 AM local) and day (8 AM – 8 PM local) for the entire summer 2015 period. Fig 3.4 shows similar ozone pollution roses restricted to the 16-30 June period over the larger study domain

(Figs. 3.4a, b) as well as in the vicinity of the Salt Lake Valley (Figs. 3.4c,d). Ozone concentrations below 55 ppb occur frequently at night in most locations (Figs. 3.4a, c) when the prevailing wind directions tend to be locally down slopes, canyons, and valleys and generally towards the GSL. For example, at rural sites at the northern and southern extents of the GSL (Locomotive Springs, LMS, and Erda, QED, respectively), land breezes directed towards the GSL are most common from 8 PM – 8 AM accompanied by ozone levels below 55 ppb (Fig. 3.4a). One deviation from this general pattern is the nighttime northeasterly winds prevailing on the western shores of the GSL at Badger Island (BGRUT) and Lakeside Mountain (O3S06) that are associated with the prevailing nocturnal mountain/plain circulation extending westward from the Wasatch Mountains across the GSL (note the prevailing winds on Fremont Island at lake level, O3S07, and at its crest, O3S08). Concentrations greater than 55 ppb are more frequent overnight at Badger Island and Lakeside Mountain than at the other rural or lake sites (Fig. 3.4a).

Pronounced nocturnal downslope and down-valley circulations accompanied by low ozone levels prevail in the Salt Lake Valley as well (Fig. 3.4c). However, the high elevation sites (Farnsworth Peak, FWP, in the Oquirrh Mountains and Snowbird, S2OZN, in the Wasatch Mountains) are often exposed to ozone levels greater than 55 ppb during the 8 PM – 8 AM period, indicative of the higher "background" ozone levels prevailing over the region.

The wind roses for the 8 AM – 8 PM period tend to exhibit locally up slope, canyon, and valley flows and generally away from the GSL (Figs. 3.4b,d). Since ozone levels usually peak during late afternoon, higher ozone concentrations are often transported during the afternoon across the eastern and southern lake shores into the Wasatch Front, e.g., at stations to the southeast of the GSL (e.g., Syracuse, QSY, Farmington Bay, O3S02, Bountiful, QBV, and Saltaire, QSA). Local afternoon upslope flows are evident on the western (Herriman, QH3) and eastern (Mountain Meteorology Lab, MTMET) slopes of the Salt Lake Valley as well as the upvalley transport of higher ozone concentrations in Little Cottonwood Canyon (S2OZN). Since the predominant flow across the central portion of the GSL continues to be from the east-northeast during much of the day, higher ozone concentrations tend to be transported across BGRUT towards the west-southwest. At the crest of the Oquirrh Mountains (FWP located 1500 m above the GSL), winds tended to be bidirectional from the west-southwest with southeasterly winds associated with higher ozone concentrations indicative of upslope flows carrying higher ozone concentrations from the Salt Lake Valley.

3.2 UU2DVAR ozone analyses during 18 June 2015

Blaylock et al. (2016) describe the strong lake breeze front that transported high ozone concentrations down the Salt Lake Valley during the late afternoon of 18 June 2015. As illustrated in Fig. 2.3, this episode took place

during one of the Intensive Observing Periods of the GSLSO₃S during which the ozone observations at the fixed locations were supplemented by mobile observations from vehicles, TRAX, and the KSL helicopter. Figure 3.5 shows the vertical profiles of potential temperature, mixing ratio, and wind from the morning and afternoon soundings at the Salt Lake International Airport. Strong stability in the morning below 2000 m MSL is replaced in the afternoon by a deep well-mixed layer. As discussed by Blaylock et al. (2016), ~~relatively strong~~ southerly winds evident in the morning sounding contributed to convergent frontogenesis later in the day that delayed the eventual push of the afternoon northerly lake breeze evident in the afternoon sounding below 200 m AGL.

A nominally west to east cross section of ozone concentration and wind direction from the crest of the Oquirrh Mountains to the Wasatch Mountains on the eastern side of the Salt Lake Valley is shown in Fig. 3.6. Ozone concentrations in both mountain ranges remained between 60-70 ppb throughout the day, indicating in a crude sense the ambient ozone levels. At Neil Armstrong Academy (NAA) on the western edge of the urban core of the Salt Lake Valley, ozone levels are very low over night and remain around 60 ppb through much of the day. As discussed by Blaylock et al. (2016), a strong lake breeze front passed NAA at ~1600 MDT and passed the Mountain Meteorology Lab (MTMET) at 1700 MDT leading to abrupt increases in ozone to ~80-90 ppb.

Ozone concentration and vector wind analyses from 0600-2300 MDT 18 June 2015 are shown in Fig. 3.7. In order to focus where ozone data are more abundant, the plotting domain is reduced from the full analysis domain shown in Fig. 1.1, e.g., restricted on the north to where the causeway crosses the main portion of the Great Salt Lake. Ozone concentrations from the fixed and mobile platforms are displayed as well in order to help diagnose the features of the ozone analyses.

During the early morning (06-08 MDT), ozone concentrations are low (< 30 ppb) below 1500 m extending northward from the Salt Lake Valley along the Wasatch Front to the east of the GSL. Observations from the fixed sites as well as from the light rail car on the Green TRAX line and several vehicles traveling to the east of the GSL help to generate these analyses. The upper reaches of the Salt Lake Valley (~1500 m ASL, the lowest elevation contour) tend to have concentrations 10-15 ppb higher than those at lower elevations. The ozone concentrations above 2000 m ASL of ~50 ppb in the Oquirrh Mountains to the west and ~60 ppb in the Wasatch Mountains to the east of the Salt Lake Valley are strongly constrained in the analysis by the observations at Farnsworth Peak (FWP) and Snowbird (S20ZN), respectively. Down slope and valley winds tend to dominate with relatively strong easterly cross-lake flow evident in the central GSL as well.

During the late morning (09-11 MDT), ozone levels increase, most notably by 11 MDT to the southeast of the GSL to the north of the Salt Lake

Valley. One of our vehicles transiting the GSL causeway at the northern edge of the figures highlights how concentrations over the GSL in that region are lower than those observed by another vehicle transiting the narrow corridor between the GSL and the Wasatch Mountains. Southerly winds down the Salt Lake Valley continue during this period while northerly winds begin to develop over the main portion of the GSL.

Ozone concentrations during midday (12-15 MDT) continue to rise particularly between Antelope Island and the Wasatch Mountains. Concentrations tend to remain lower across the causeway to the north. Southerly winds continue in the southern half of the Salt Lake Valley while the lake breeze begins to penetrate into its northern reaches.

During the next 2 hours (16-17 MDT), ozone observations from the KSL helicopter supplement the other observations. The sensitivity tests described in Chapter 2 are performed for 16 MDT when the helicopter and other mobile observations help define the sharp contrast in ozone concentrations across the lake breeze front at that time. Due to the lack of observations over the lake itself, the UU2DVAR analysis at 16 MDT likely underestimates the ozone concentration over the southern lake then as suggested by the observations on the western shore at Badger Island (BGRUT) and to the southwest of the lake at Saltaire (QSA). Higher ozone concentrations are apparent behind the lake breeze front in the Salt Lake Valley and lower levels in front of it. Those

gradients are even stronger in the Salt Lake Valley during the next hour, 17 MDT (Blaylock et al. 2016).

The position of the lake breeze front at 18 MDT is broadly consistent with the radial velocity data from the Salt Lake Terminal Doppler Weather Radar and other observations (Blaylock et al. 2016). Ozone concentrations in the central and southern Salt Lake Valley are now higher than those further north. Westerly flow towards the Wasatch Mountains at 18-19 MDT is consistent with the peak ozone concentrations observed at Snowbird at 19 MDT. The late evening helicopter transects at 20-21 MDT help to define the lowering ozone levels with increasing titration evident after sunset (22-23 MDT). Ozone levels remain higher at Snowbird and Farnsworth Peak during this period.

Overall, the UU2DVAR analyses help to define and unify many of the temporal and spatial features evident in the disparate sources of ozone observations. However, there are also noticeable non-physical artifacts introduced by how the background fields are defined and the bogusing of the lakeshore observations over the lake. For example, since the Snowbird observation is the only one available in the Wasatch Mountains unless the helicopter traverses them, its concentrations largely defines what is analyzed in those mountains. Obviously artificially smooth geometric shapes are present at times over the GSL. Those often arise when there are large discrepancies between the background concentration based on the median of the available

lakeshore observations and individual lakeshore observations that are bogused over the lake. Sharp discontinuities across the lake shore are also introduced as a result of the assumption to minimize observations over the lake from influencing those onshore and vice versa. These types of issues have been difficult to overcome for other variational analyses such as the Real Time Mesoscale Analysis (Tyndall and Horel 2010).

3.3 UU2DVAR ozone analyses during 27 June 2015

The spatial and temporal evolution of ozone and surface wind is now examined for 27 June 2015 when the greatest number of exceedances of the 70 ppb NAAQS 8-hr standard during the summer was observed (Fig. 3.2). Figure 3.6 highlights that the boundary layer tended to be warmer with lighter morning down valley flow and afternoon lake breeze on this day relative to that on 18 June.

Using the same pseudo cross section used for the previous case, the ambient background ozone levels on this day are ~10 ppb higher than those on 18 June (Fig. 3.6). Nocturnal titration drove ozone levels to near 0 ppb at NAA increasing to over 80 ppb later in the day while peak ozone concentrations at QHW and MTMET were over 100 ppb. Those peak concentrations occurred earlier in the day since the lake breeze was not delayed as it was on 18 June. Of particular note is the peak 90 ppb concentration at Snowbird reached at 18 MDT.

As shown in Fig. 3.9, ozone concentrations during the early morning hours (06-09 MDT) are broadly similar to those on 18 June with low values below 1500 m in the urban areas and higher values at Farnsworth Peak and Snowbird. The only mobile asset on this day supplementing the fixed site observations is the sensor onboard the light rail car traversing the red line in the Salt Lake Valley. The winds during the early morning are again for the most part down slope and down valley with the easterly winds across the GSL's central core.

Ozone levels increase throughout this region during the late morning. By solar noon (13 MDT), they are analyzed to be over 70 ppb over the GSL with even higher concentrations to its southeast. A well-defined lake breeze extends southwestward into the Salt Lake Valley accompanied by the high ozone levels. During midafternoon (14-16 MDT), ozone concentrations tend to increase throughout the domain, including at the high elevation sites, Farnsworth Peak and Snowbird. The highest ozone concentrations are observed along the western lakeshore at Badger Island and nearby Lakeside Mountain (O3S06, not shown as it lies off the western edge of the figure) as well as Erda (QED) in the Tooele Valley directly to the south of the GSL and Saltaire (QSA) near its southwestern shore. Increasing ozone levels observed at Snowbird led to the highest concentrations analyzed in the Wasatch Mountains at 18 MDT. Ozone levels then dropped sharply during the late evening and early night hours.

As mentioned regarding the analyses completed for 18 June, some artificial features are apparent in the analyses, particularly the lower concentrations over the southern portions of the GSL relative to the lakeshore at 15 MDT. However, overall the ozone analyses help to integrate the available ozone observations such that the critical spatial and temporal changes become evident as the day progresses.

3.4 Composite diurnal variation in ozone during 16-30 June 2015

As a means to examine the "typical" evolution of ozone during days that experience high ozone levels, Figure 3.10 shows the averages over 3-hr blocks of the hourly ozone and surface wind analyses during the 16-30 June 2015 period. These composite ozone analyses depend on all of the available fixed site observations as well as all of the intermittent mobile observations available at times during this period. Average ozone concentrations within those 3-hr intervals at each fixed site are also shown in Fig. 3.10. Using as a reference the averages of the Farnsworth Peak observations in the Oquirrh Mountains as an indicator of the free-atmosphere ozone concentrations, the background ozone levels throughout the day vary by a limited amount, remaining between 50 and 60 ppb. Composite ozone levels at Snowbird in the Wasatch Mountains downwind of the Salt Lake Valley tend to be higher, between 60-70 ppb. Much larger diurnal swings (20-70 ppb) are evident in some of the lowest elevations of the Wasatch Front.

Both the station averages and the composite analyses illustrate the general tendency for the lowest and highest concentrations to take place in the urban corridor of the Wasatch Front. Lakeshore observations and the resulting analyses over the main body of the GSL suggest that the GSL may not necessarily be a reservoir of high ozone overnight nor generally during the day. The highest ozone concentrations observed and analyzed in the afternoon tend to be sandwiched between the GSL and the Wasatch Front, particularly in the Farmington Bay region.

The composite wind analyses help to define the typical diurnal wind circulations emphasizing the strong role of thermally-forced circulations arising from the lake and the surrounding terrain. Down slope and valley circulations combine with land breezes overnight in many locations. A notable exception is the relatively strong easterly flow across the central portions of the GSL from 21-08 MDT presumably resulting from the larger-scale mountain-plain circulation between the Wasatch Mountains and the GSL Basin. By midday, up slope and up valley circulations combined with lake breezes dominate these composites until sunset.

As noted earlier limitations imposed by the available observations and assumptions regarding the background error covariances can introduce artificial features in these composite analyses. For example, the differences in composite ozone across the easternmost shorelines of the GSL are likely too abrupt. This artifact can also be found in the benches at the base of the

Wasatch Mountains where strong gradients of ozone occur likely due to the abrupt change in elevation.
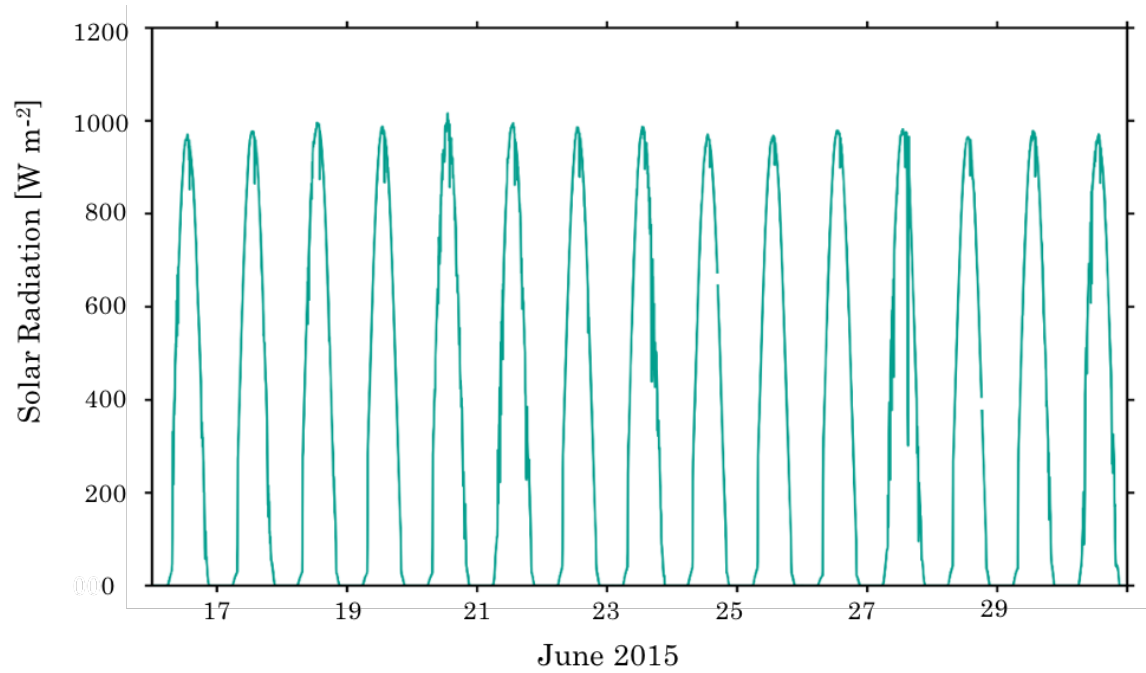
Figure 3.1 Incoming solar radiation (W m^{-2}) at the MTMET station in the Salt Lake Valley from 16-30 June 2015. See Fig. 3.4 for the location of MTMET.
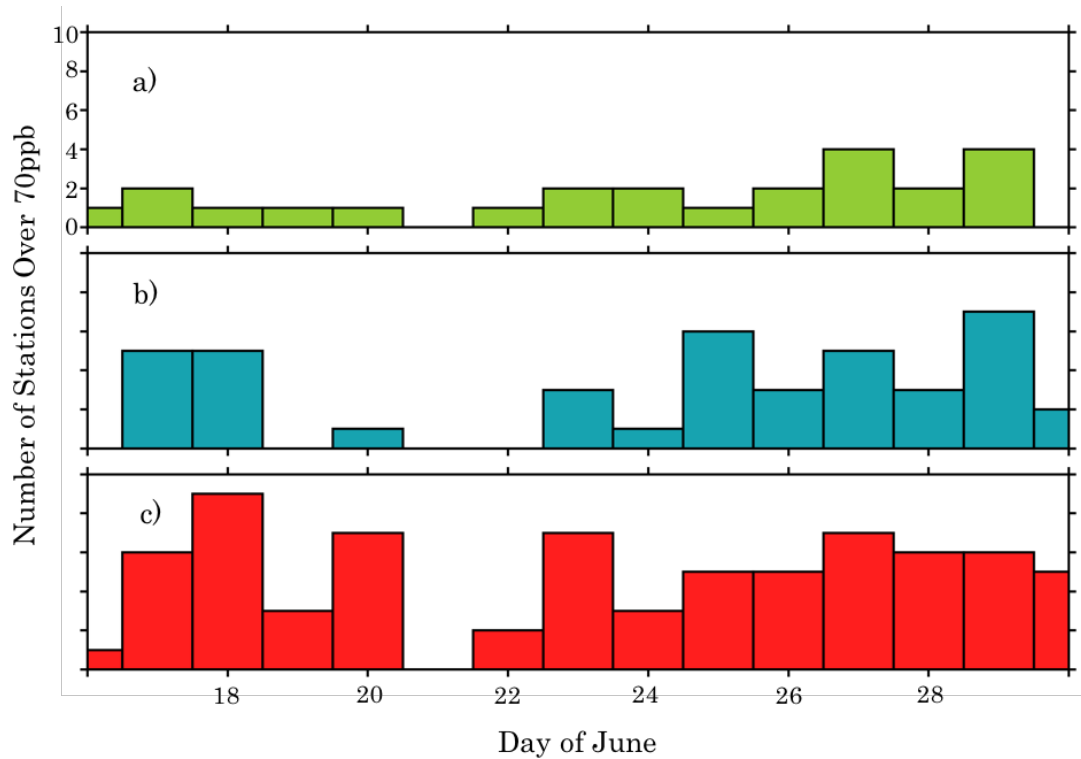
Figure 3.2. Number of stations in the a) rural, b) lakeshore, and c) urban categories from 16-30 June 2015 that exceed 70 ppb during an 8-h period categorized as follows: a) rural, b) lake, and c) urban.
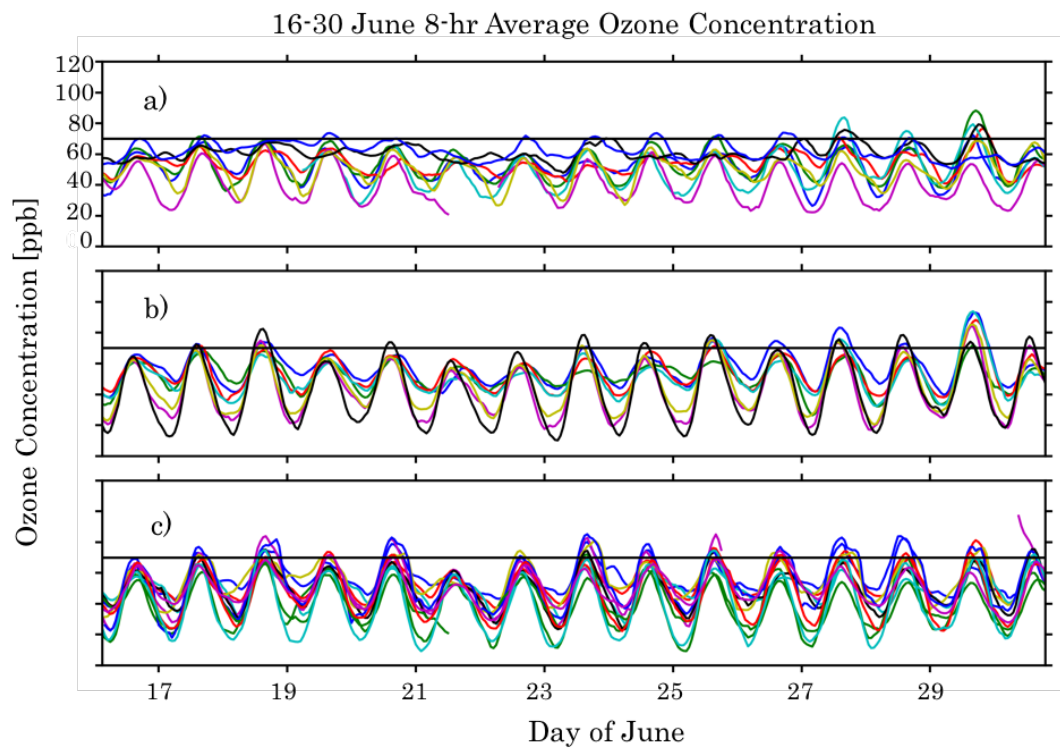
Figure 3.3. 8-hr average ozone concentrations for all stations in the a) rural, b) lakeshore, and c) urban categories from 16-30 of June. The current ozone NAAQS standard of an 8-h average of 70 ppb is denoted by the horizontal lines.

O3S02

QBV

MTMET

QSA

QHW

FWP

NAA

S2OZN

QH3
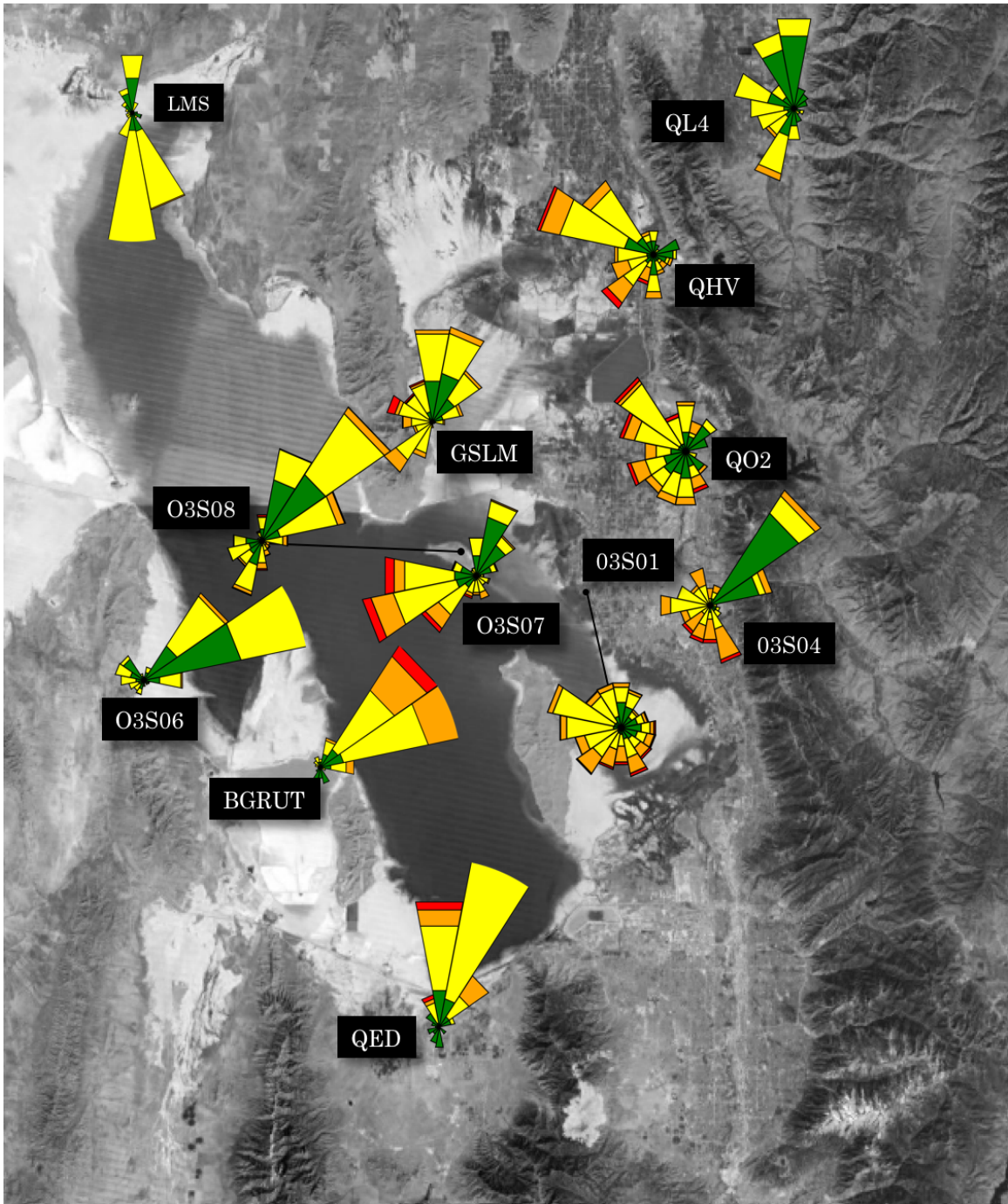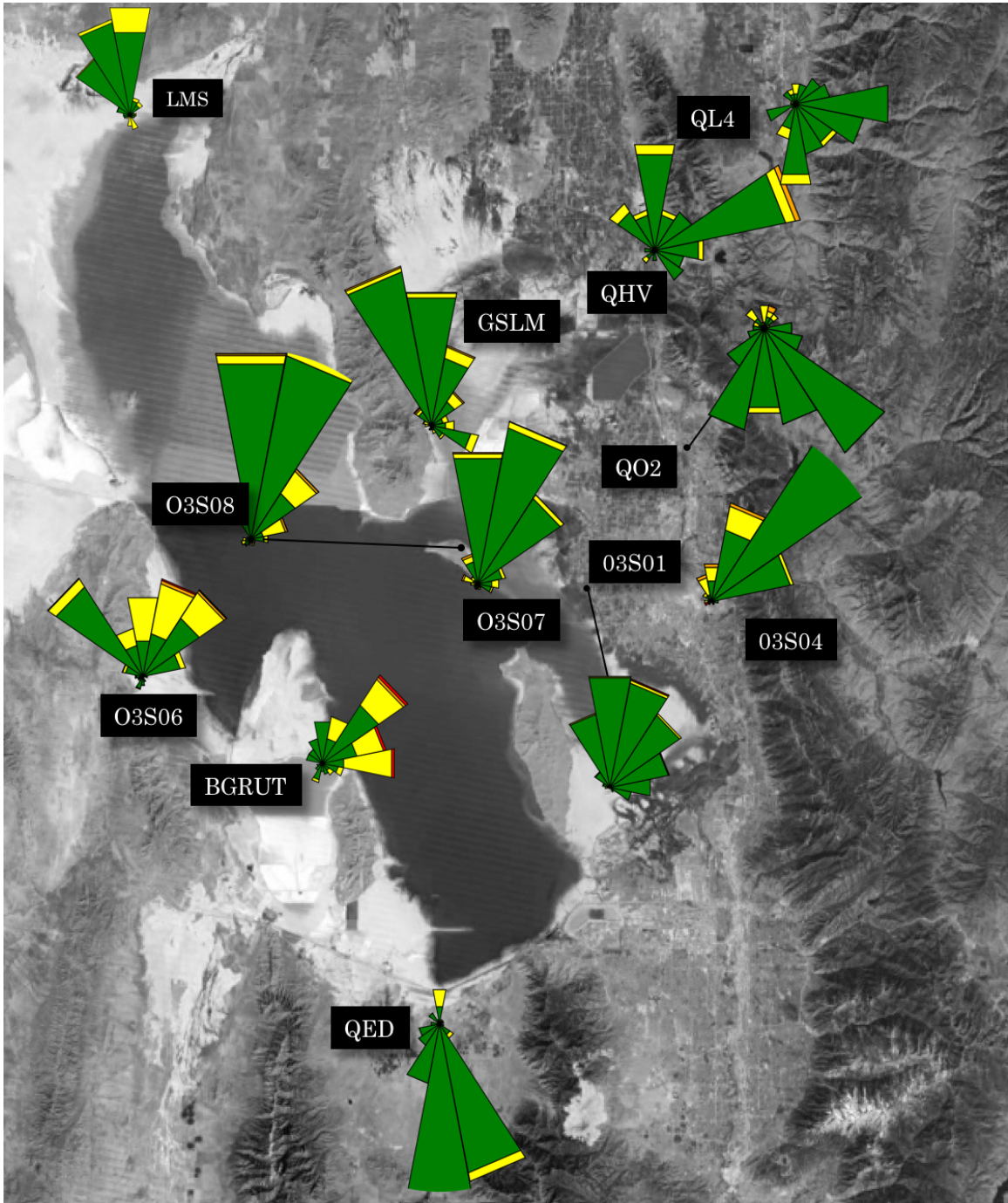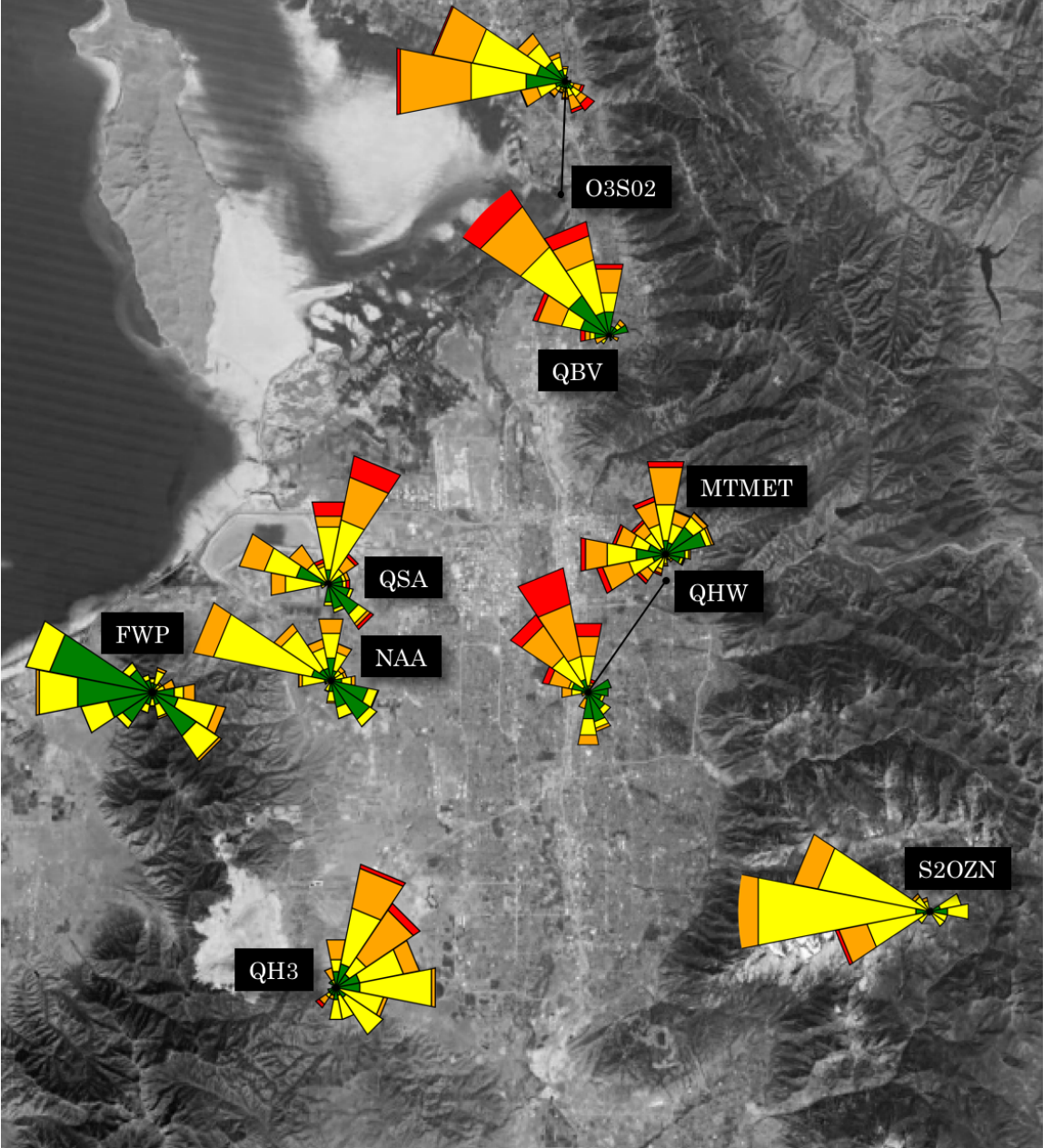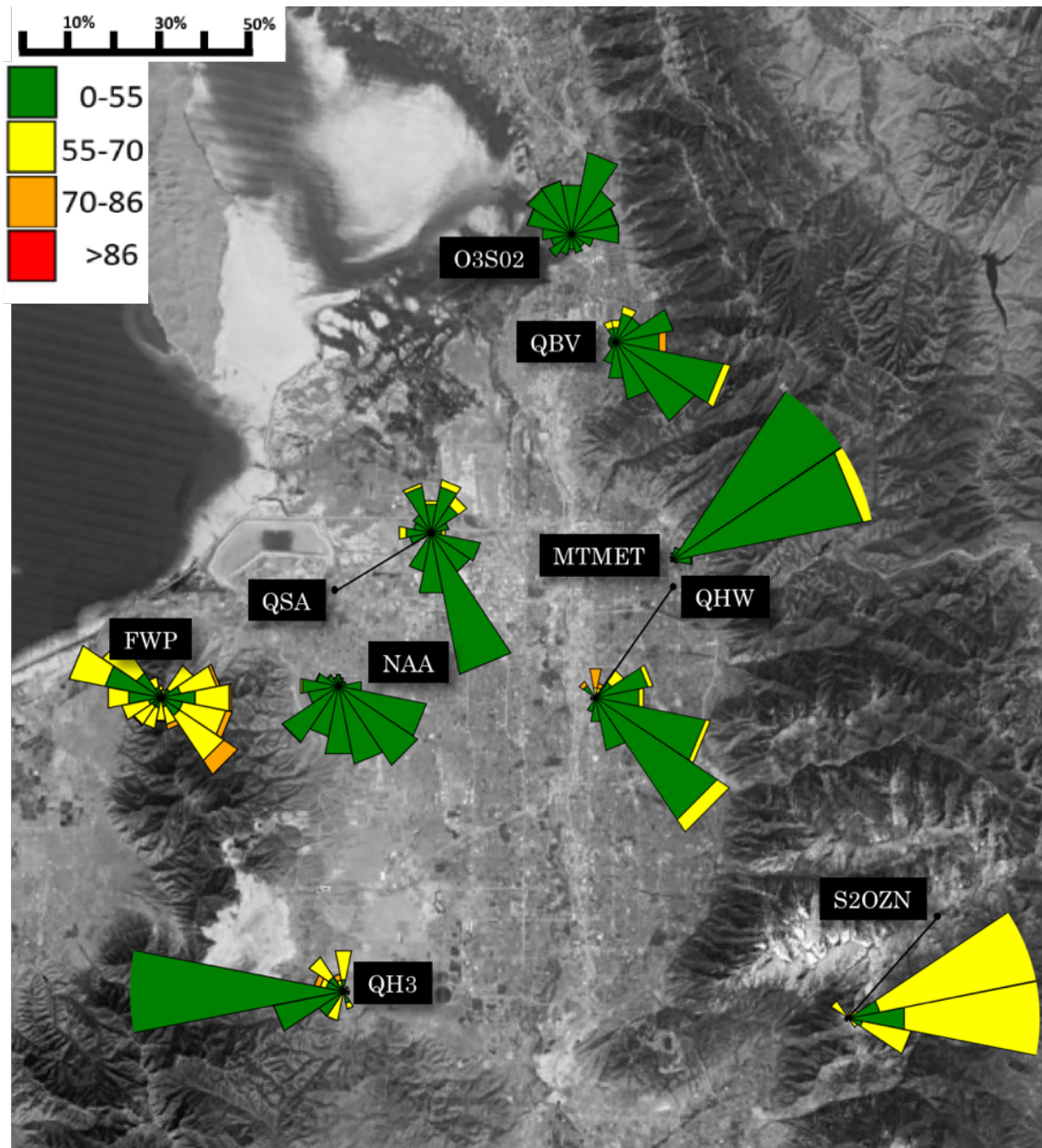
Figure 3.4. Ozone wind roses for 16-30 June 2015 during: (a,c) day (8 AM – 8 AM) and (b,d) day (8 PM – 8 AM) local time. The length of each of the 16 cardinal direction colored wedges represents the percentage of time the ozone concentrations fall within each colored range when the wind is blowing from that direction according to the scale in the upper left.
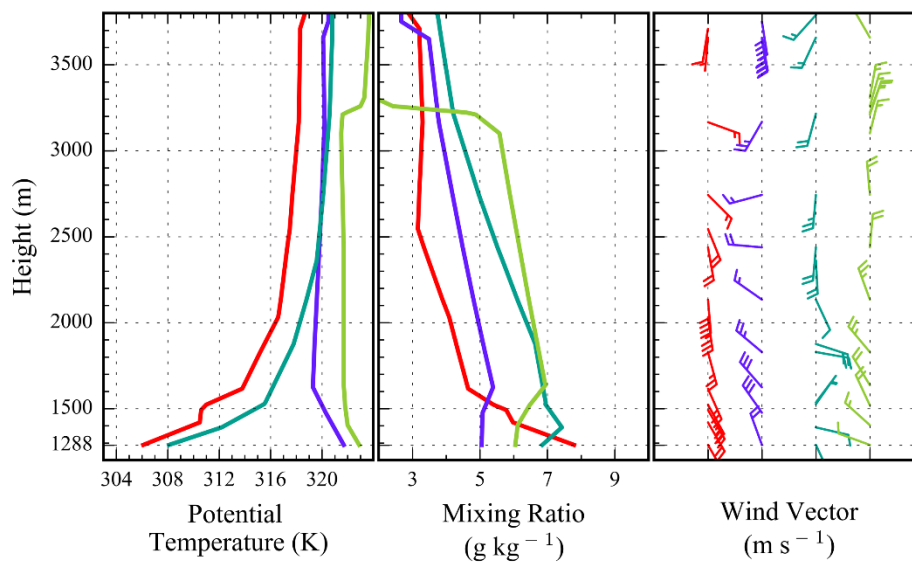
Figure 3.5. Vertical profiles of potential temperature (K), mixing ratio (g kg [-1]), and vector wind at the Salt Lake International Airport during the morning (red) and afternoon (purple) 18 June 2015 and during the morning (teal) and afternoon (green) 27 June 2015. Half and full barbs denote speeds of 1.0 and 2.0 ms^{-1}, respectively.
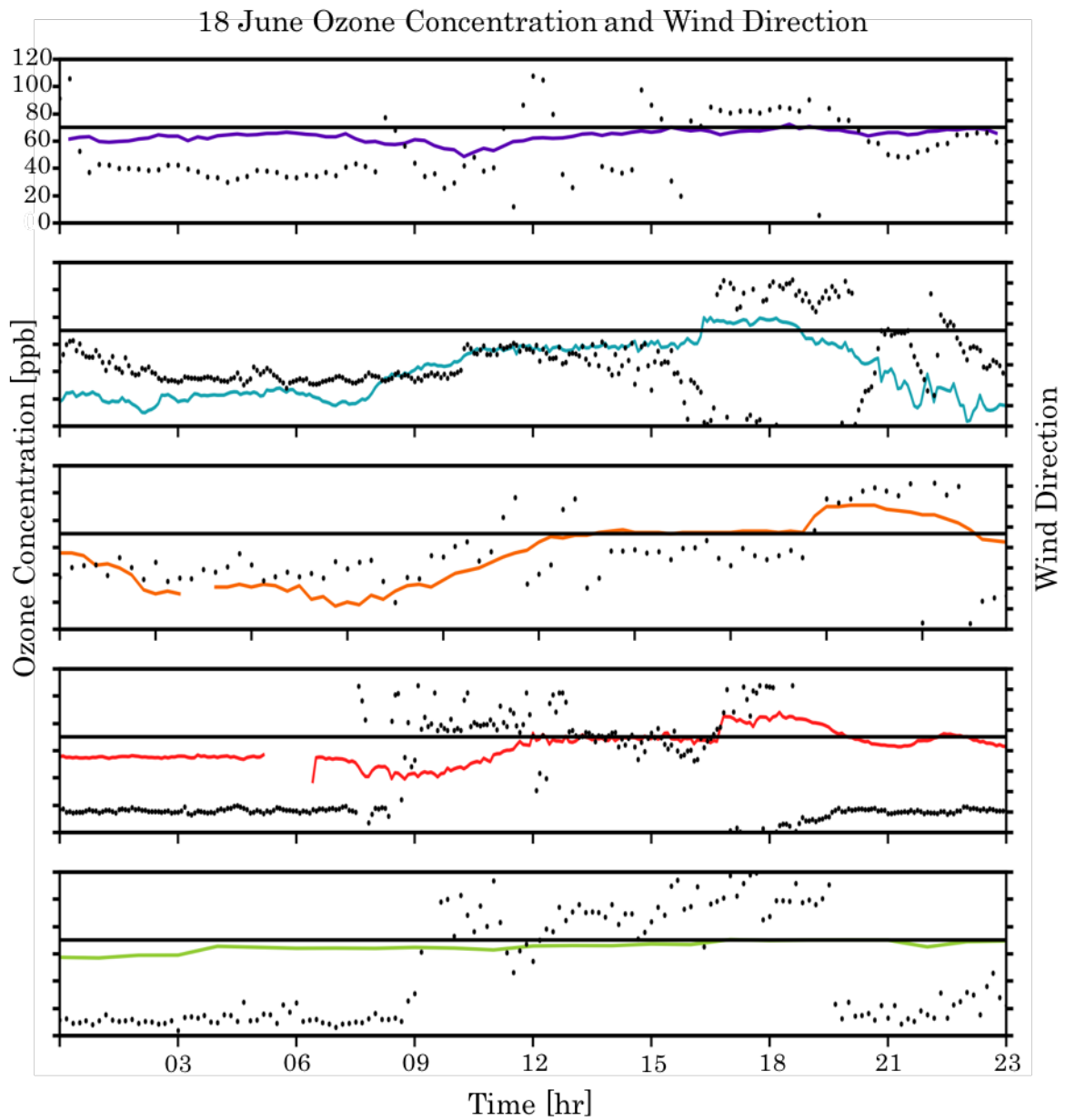
Figure 3.6. Time series of ozone (ppb) and wind direction (circles) at: a) Farnsworth Peak (FWP), b) Neil Armstrong Academy (NAA), c) Hawthorne (DAQ), d) Mountain Meteorology Lab (MTMET), and e) Snowbird (S2OZN).
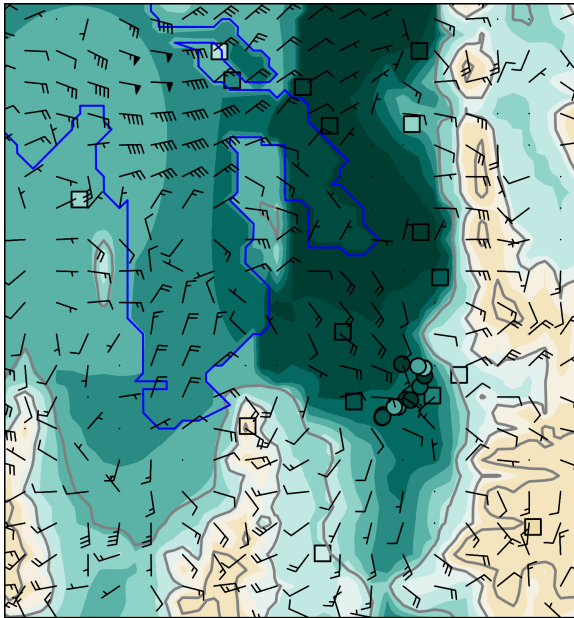
061806 MDT
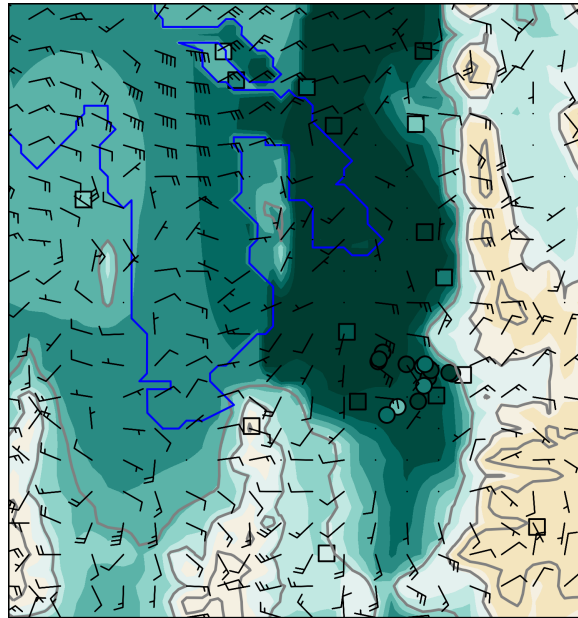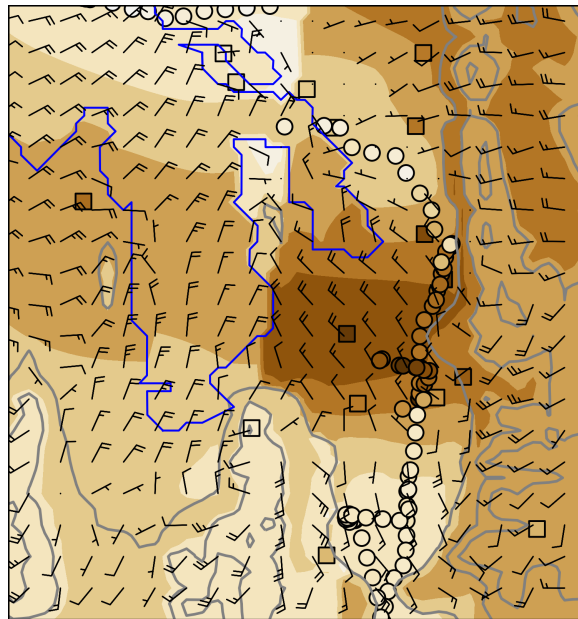
061807 MDT
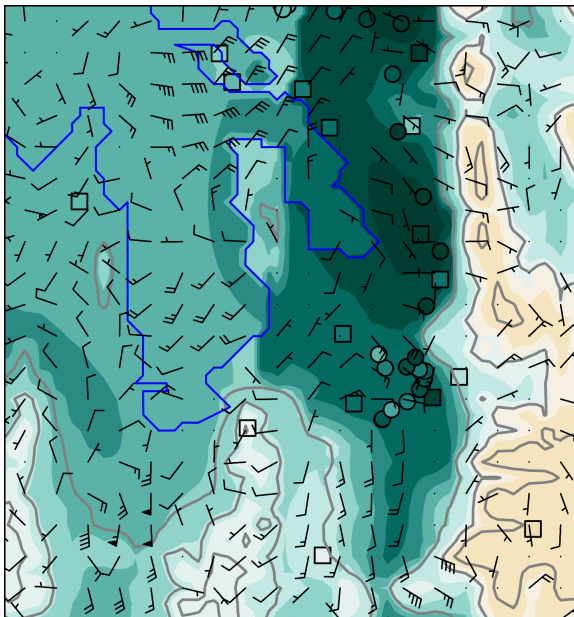
061808 MDT
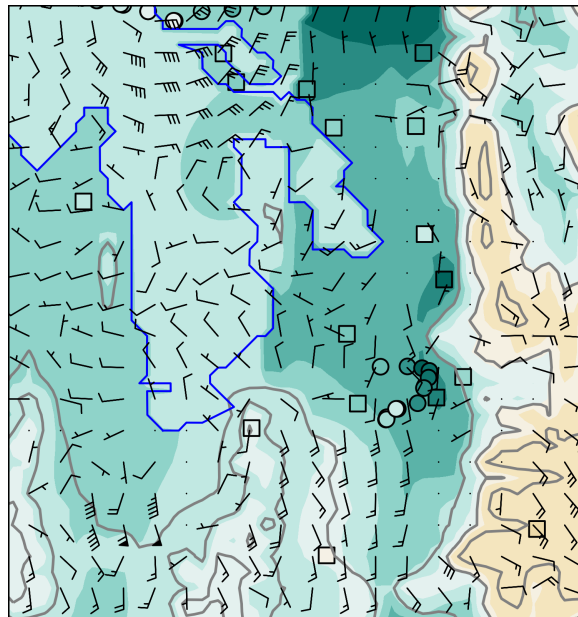
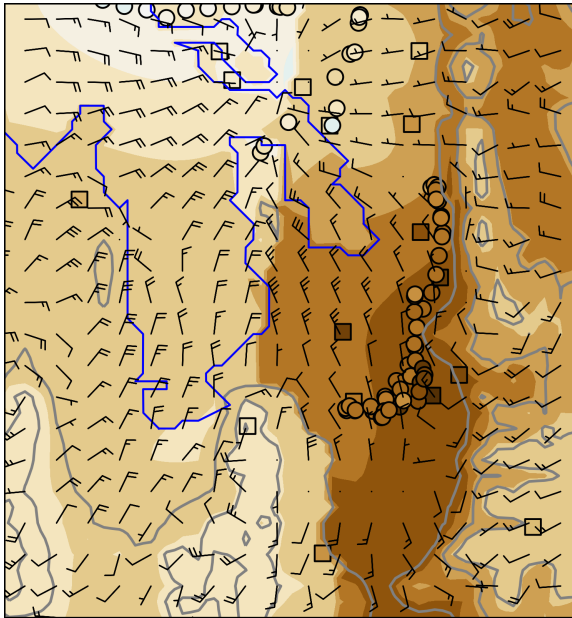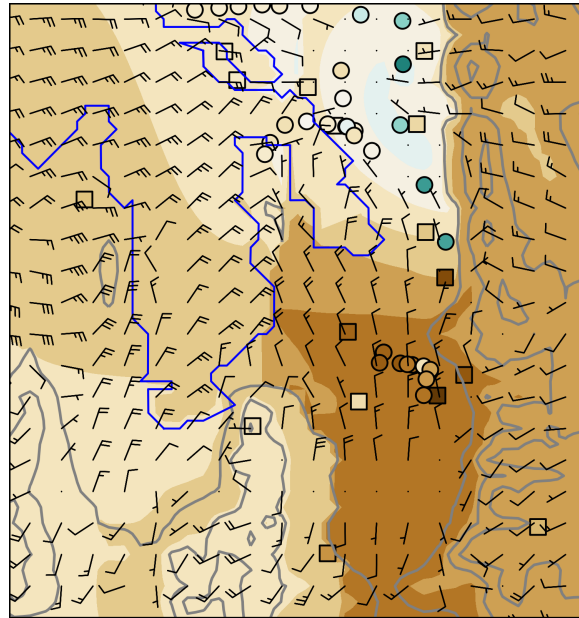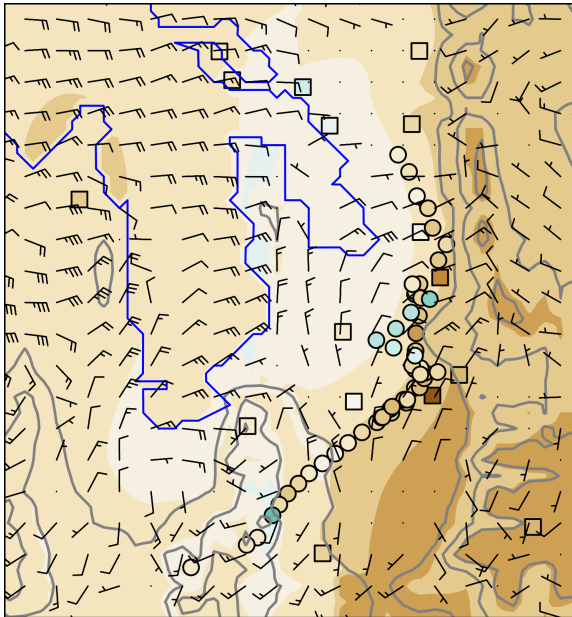061809 MDT
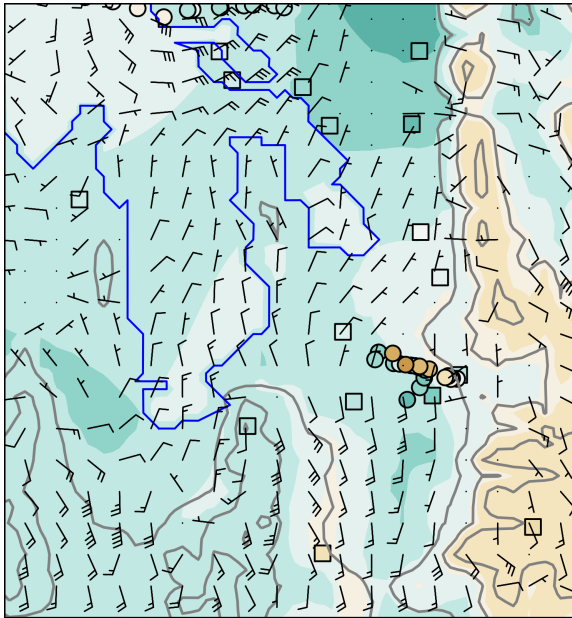
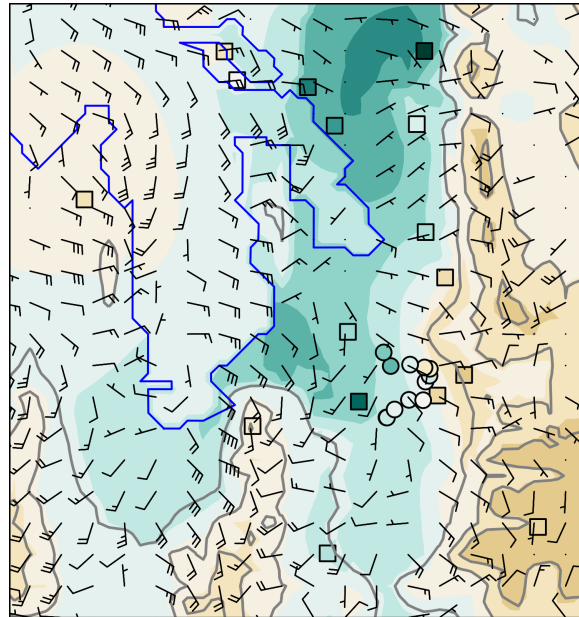061810 MDT
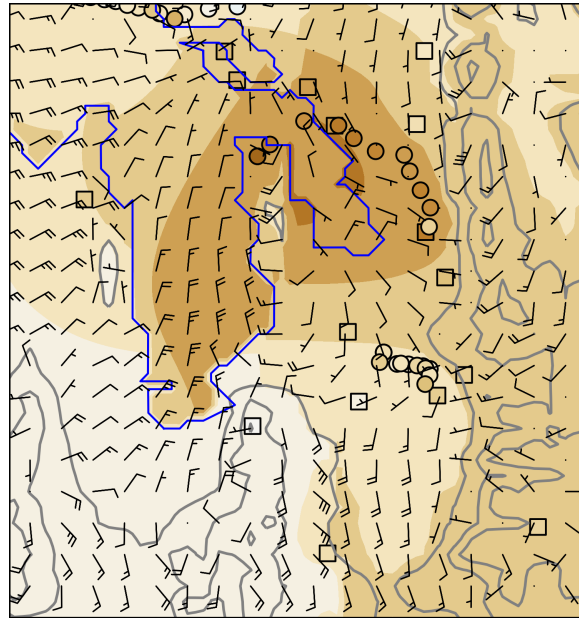
061811 MDT
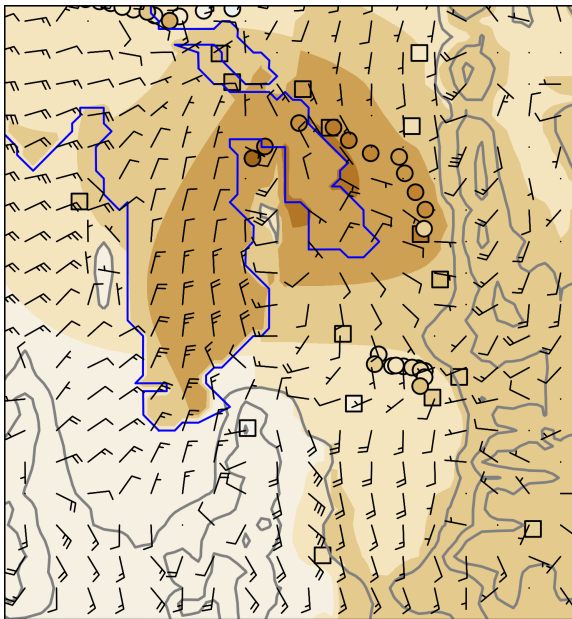
061812 MDT
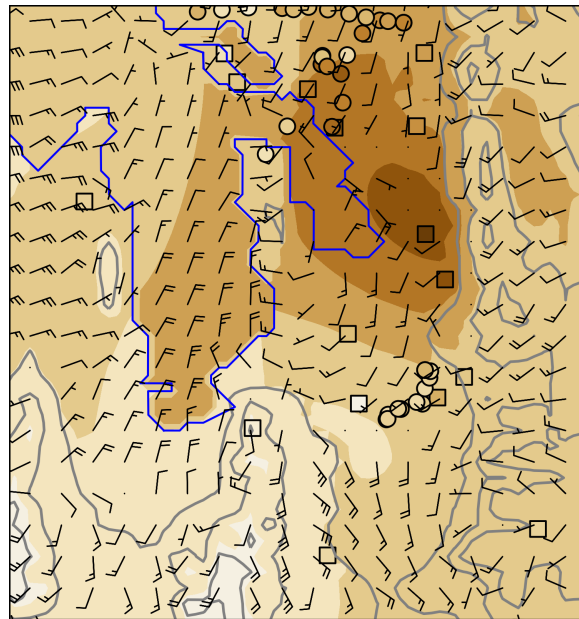
061813 MDT
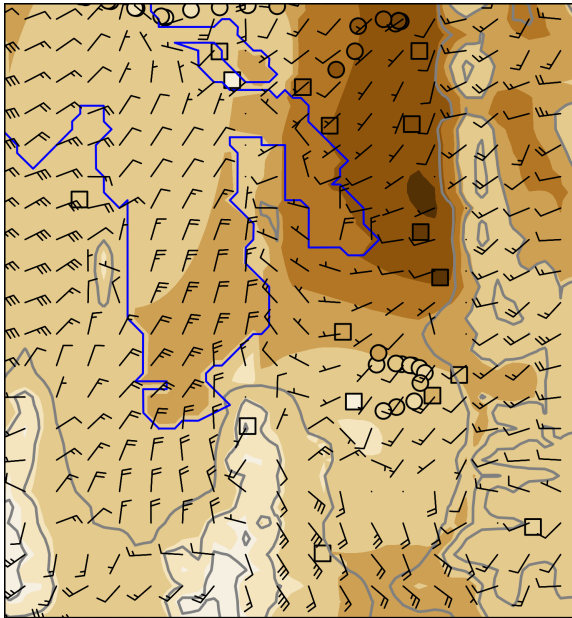
061814 MDT
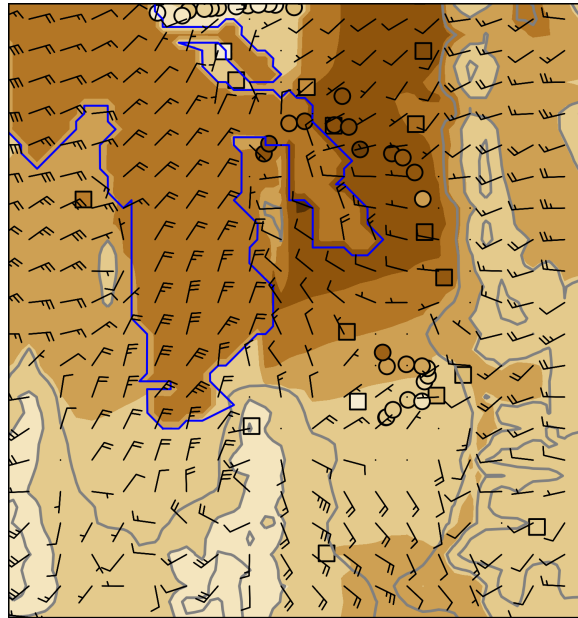
061815 MDT
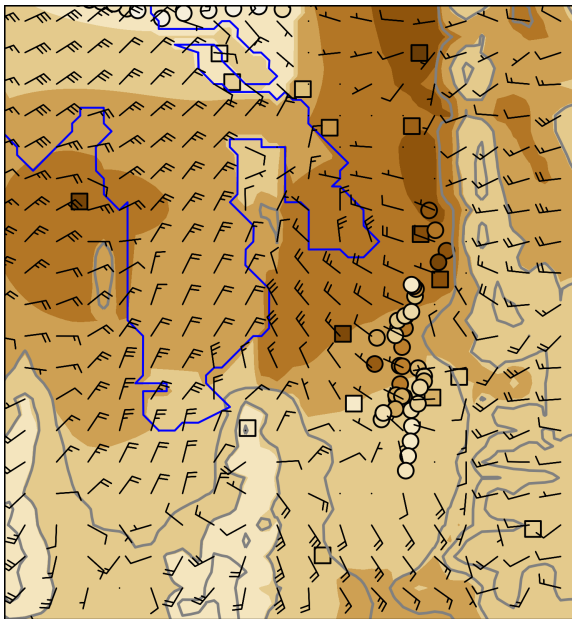
061816 MDT

061817 MDT

061818 MDT

061819 MDT

061820 MDT

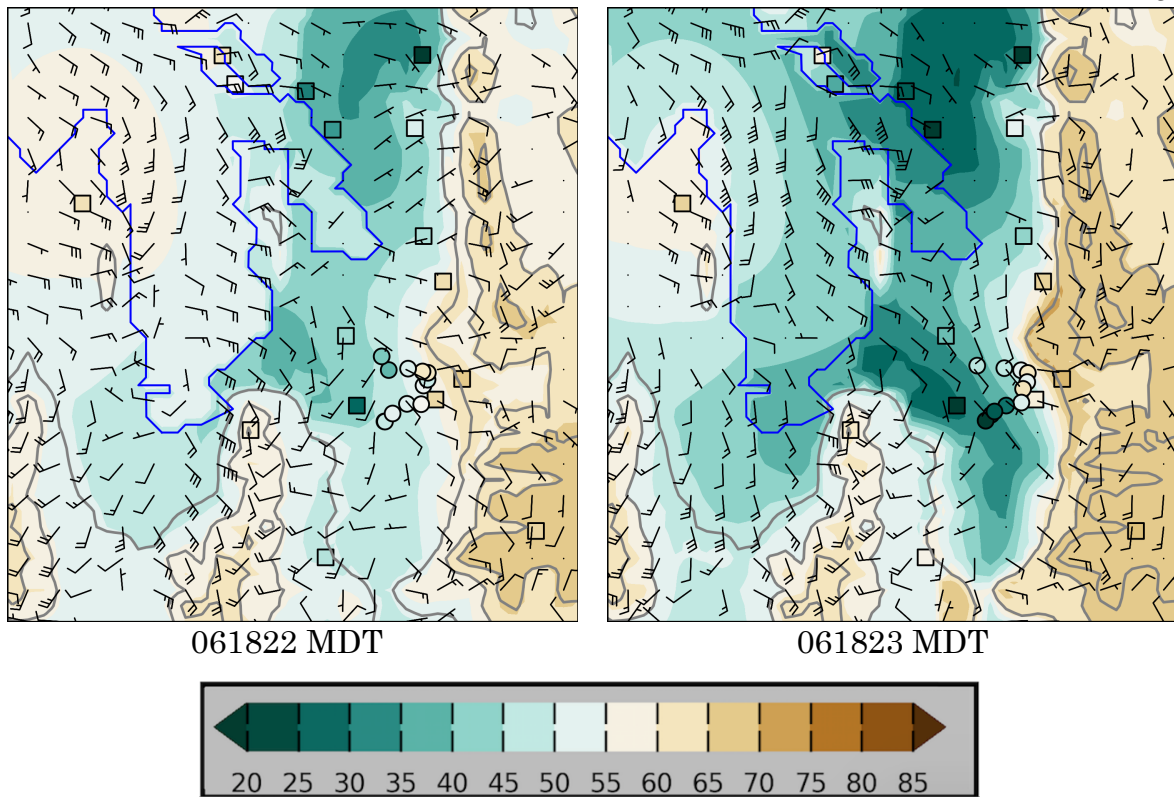061821 MDT

061822 MDT   061823 MDT

Figure 3.7. Ozone concentration analyses shaded according to the colorbar during 18 June 2015 at hourly intervals from 0600 – 2300 MDT. Vector wind analyses at every 4th gridpoint superimposed where half and full barbs denote speeds of 1.0 and 2.0 m s^{-1}. Observations of ozone concentrations at fixed sites (squares) and from mobile observations (circles) are shown using the same colorbar. Elevation contoured in light grey at 500 m intervals beginning at 1500 m.
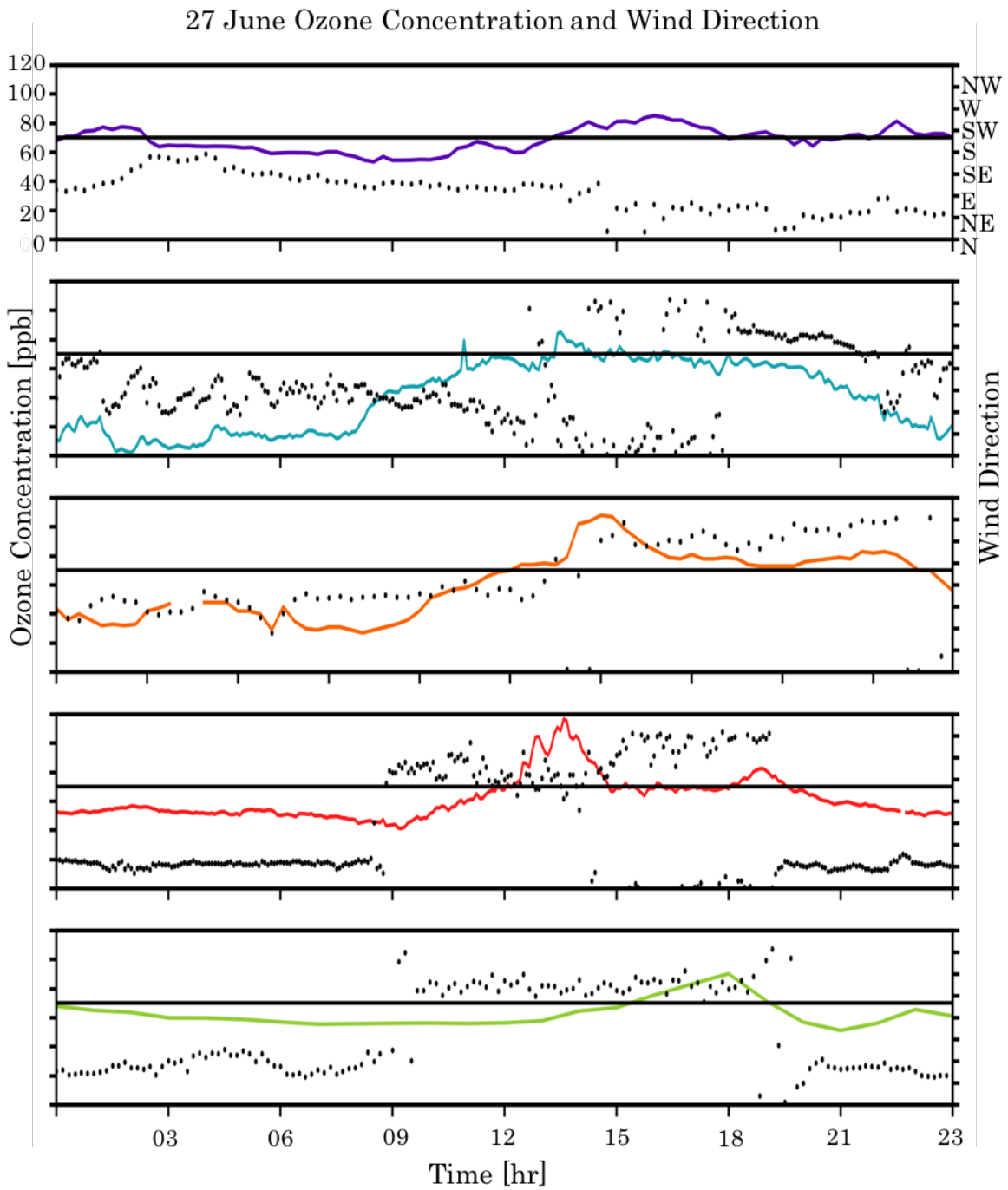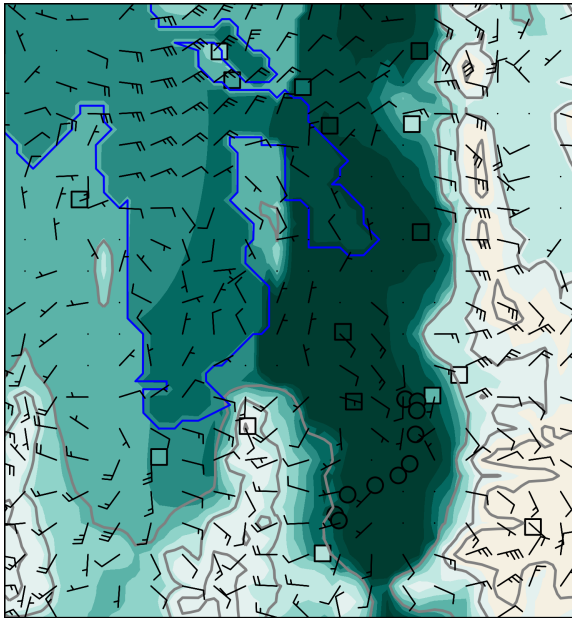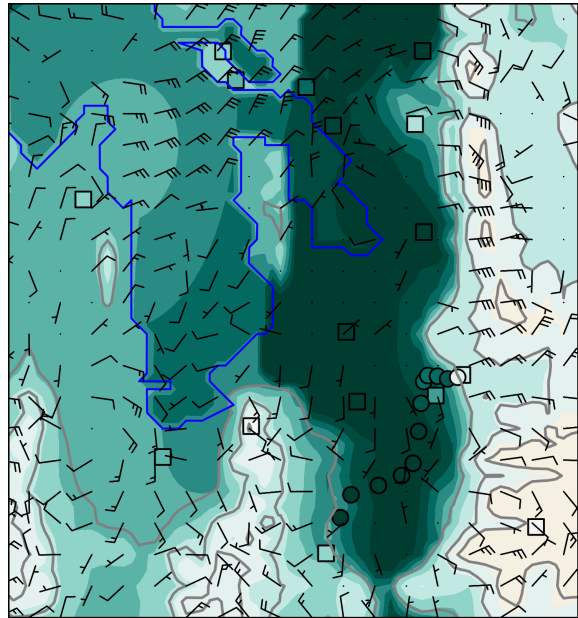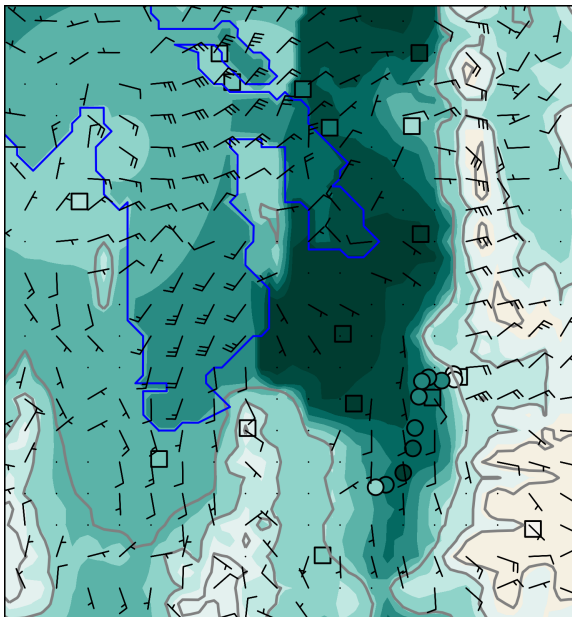
Figure 3.8. Time series of ozone (ppb) and wind direction at: a) Farnsworth Peak (FWP), b) Neil Armstrong Academy (NAA), c) Hawthorne (DAQ), d) Mountain Meteorology Lab (MTMET), and e) Snowbird (S2OZN).

062706 MDT

062707 MDT

062708 MDT
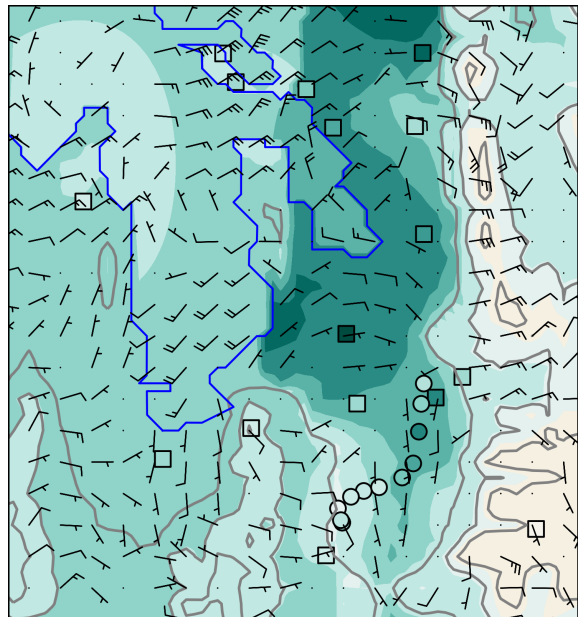
062709 MDT
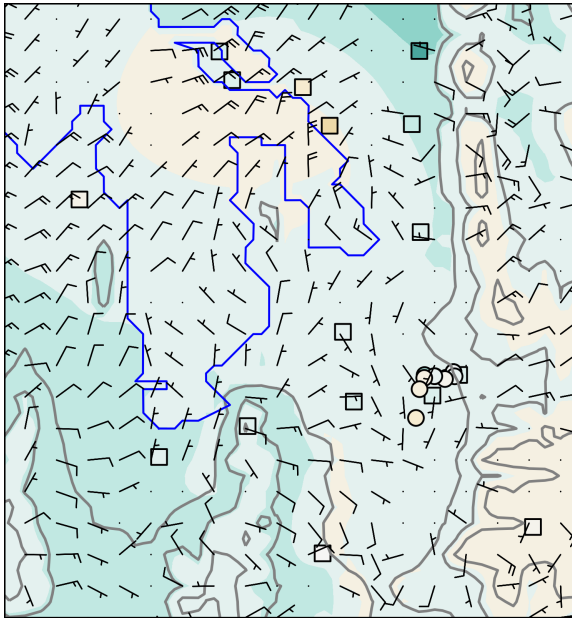
062710 MDT
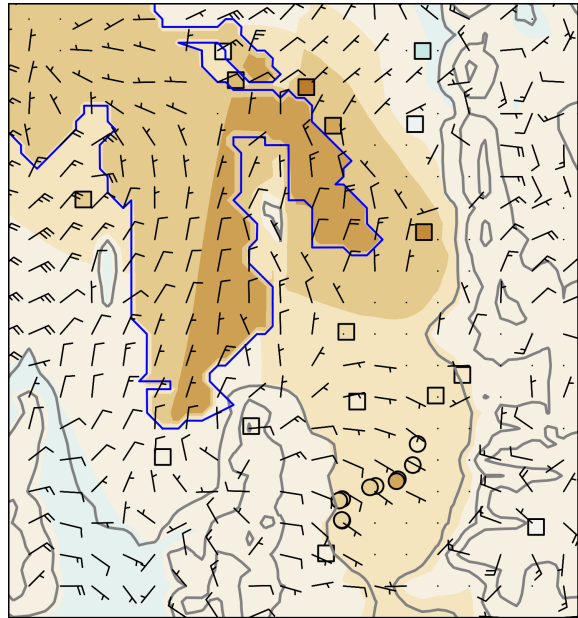
062711 MDT
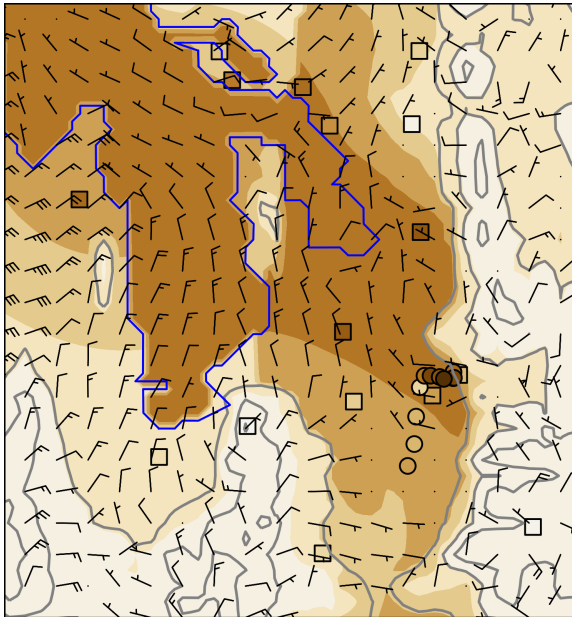
062712 MDT
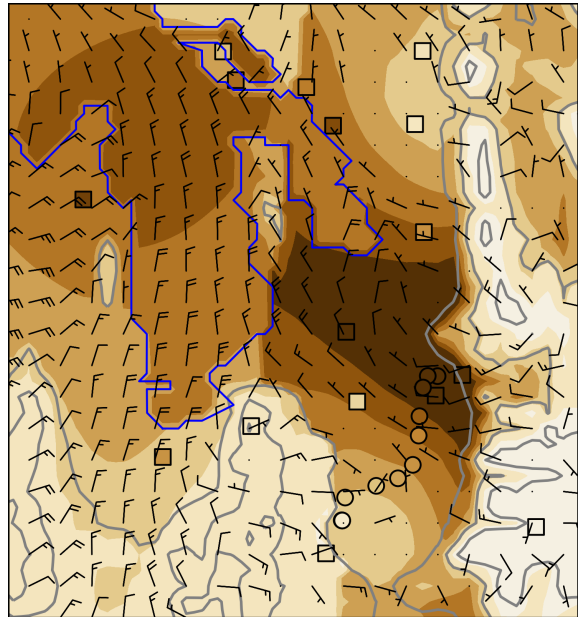
062713 MDT
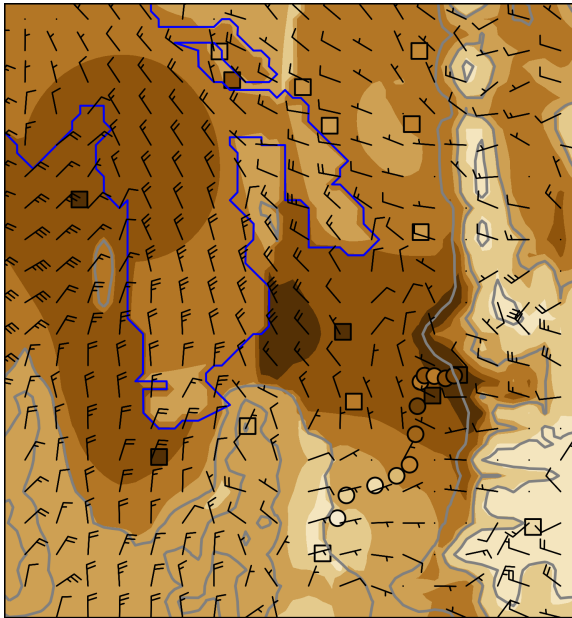
062714 MDT
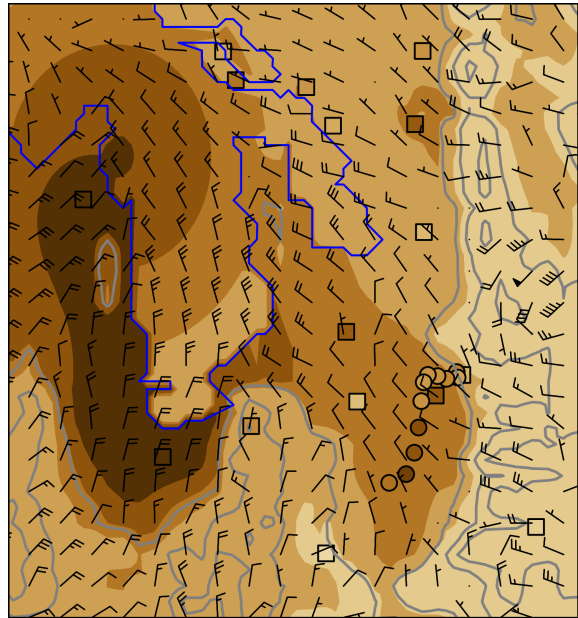
062715 MDT
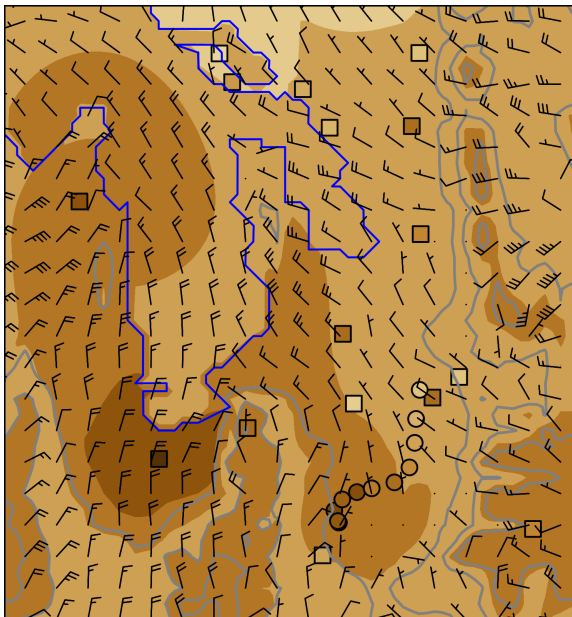
062716 MDT
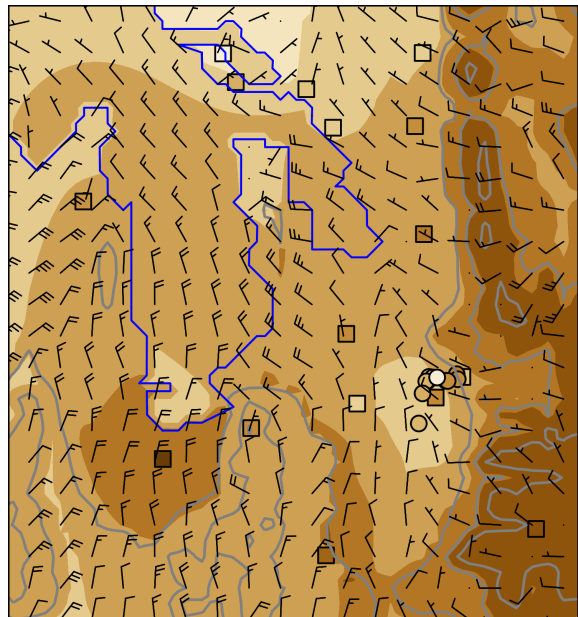
062717 MDT
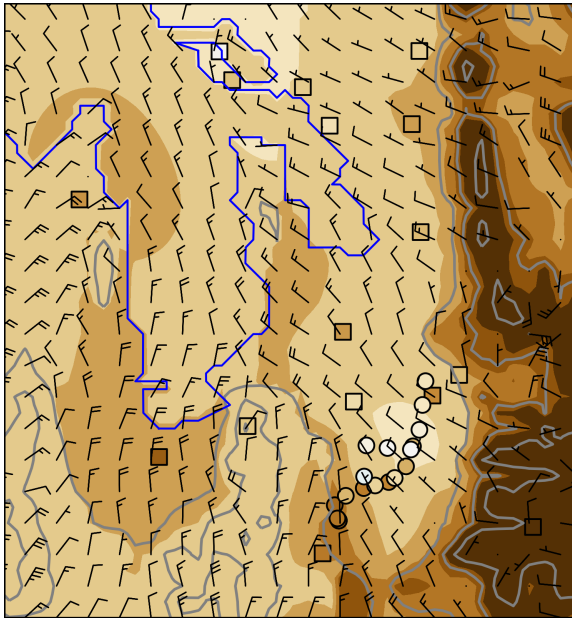
062718 MDT
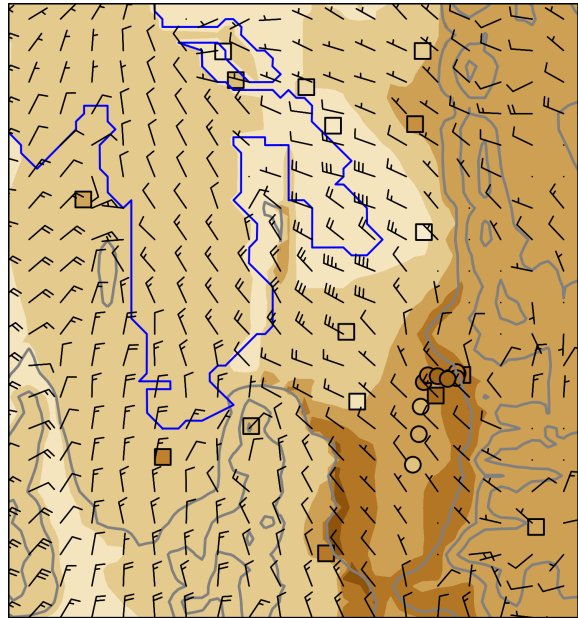
062719 MDT
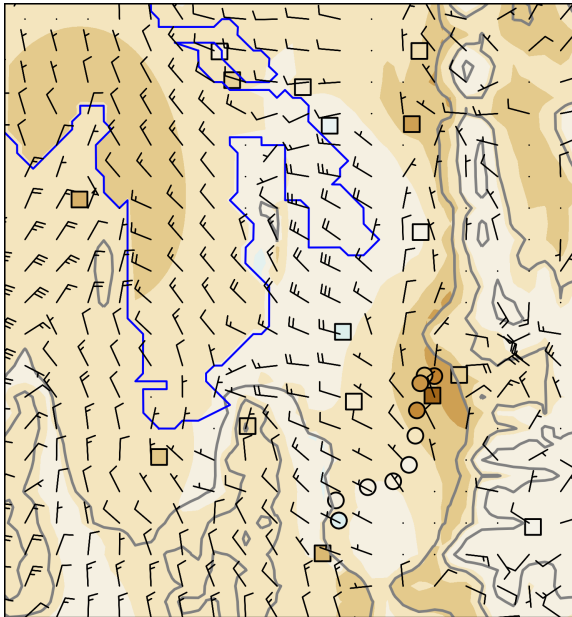
062720 MDT

062721 MDT
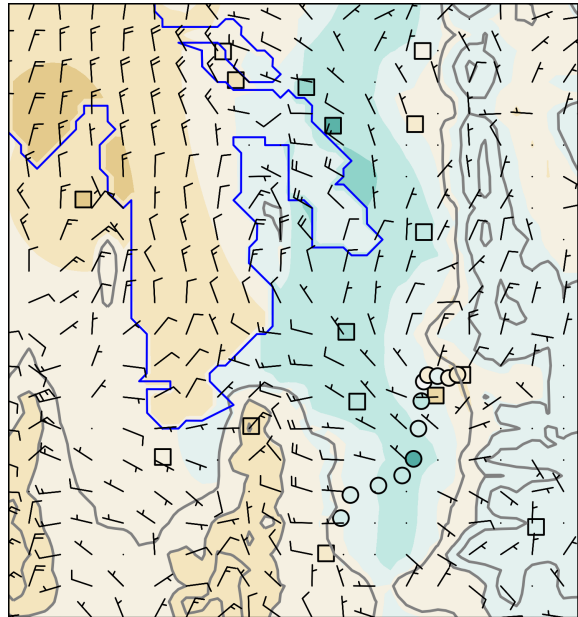
062722 MDT 062723 MDT
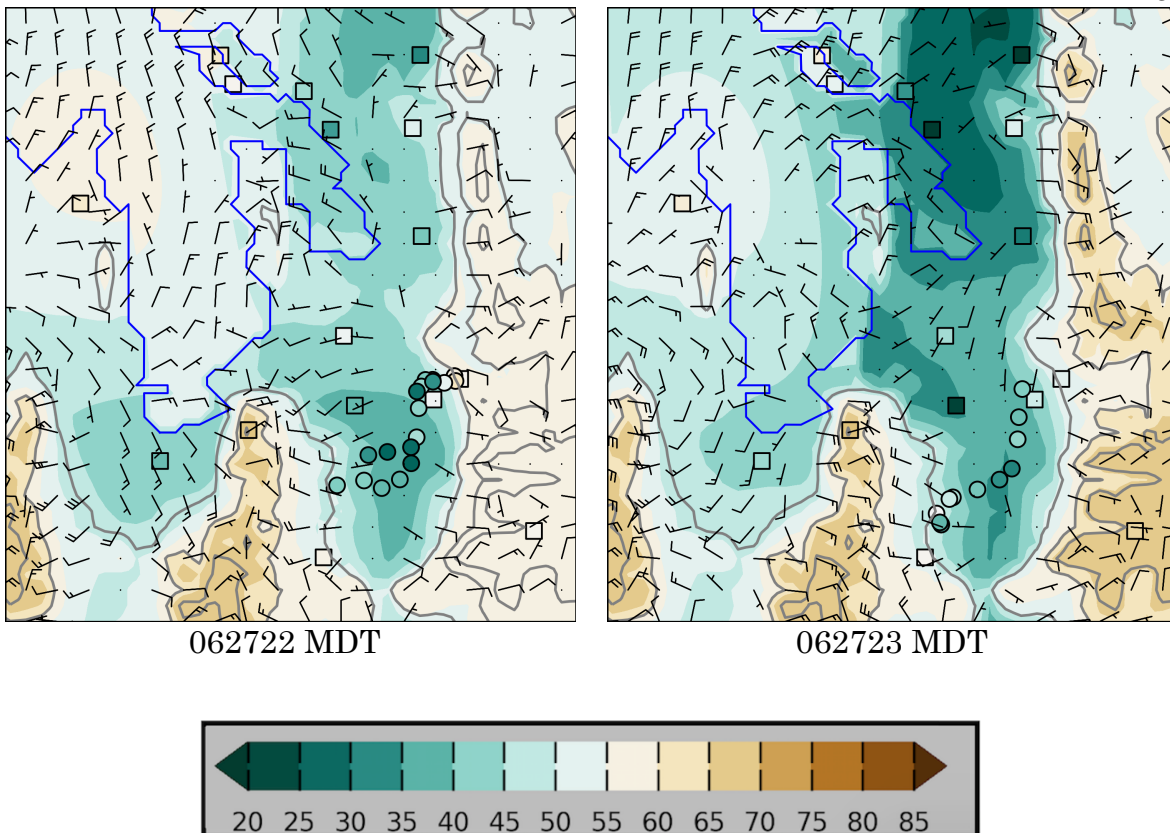
Figure 3.9 Ozone concentration analyses shaded according to the colorbar during 27 June 2015 at hourly intervals from 0600 – 2300 MDT. Vector wind analyses at every 4th gridpoint superimposed where half and full barbs denote speeds of 1.0 and 2.0 m s^{-1}. Observations of ozone concentrations at fixed sites (squares) and from mobile observations (circles) are shown using the same colorbar. Elevation contoured in light grey at 500 m intervals beginning at 1500 m.
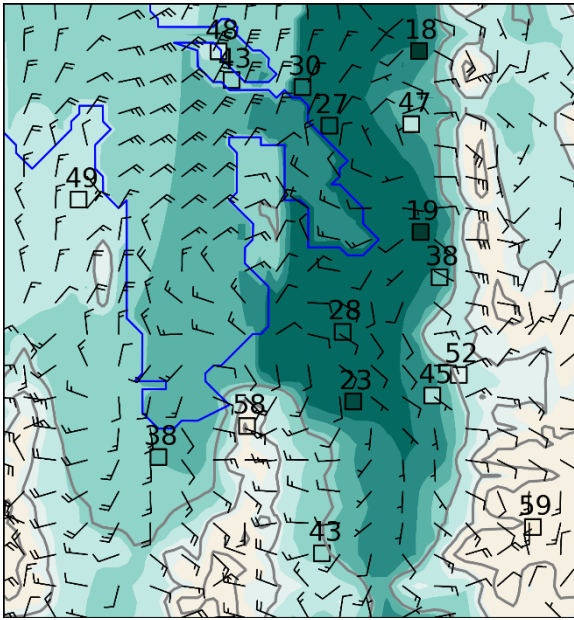
00-02 MDT
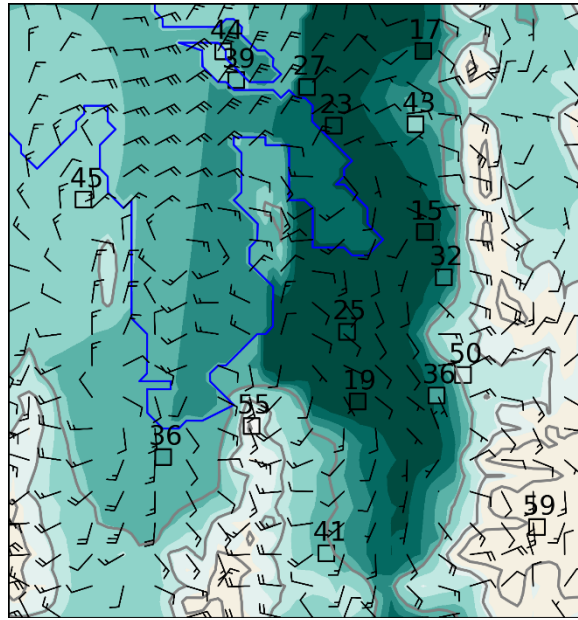
03-05 MDT

06-08 MDT

09-11 MDT

12-14 MDT

15-17 MDT

18-20 MDT
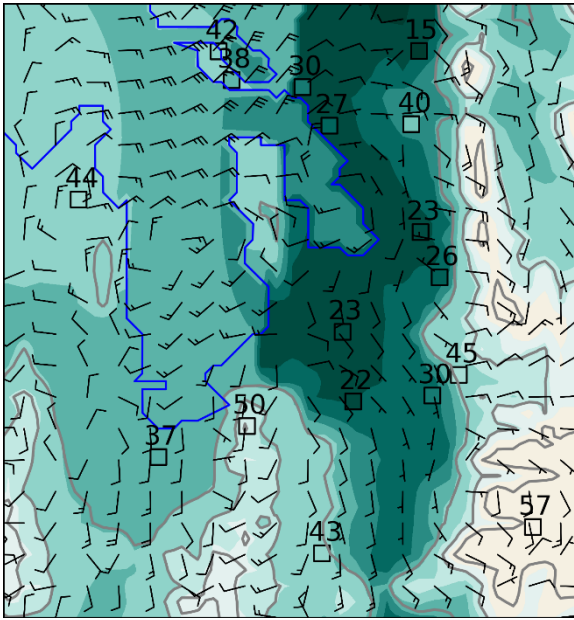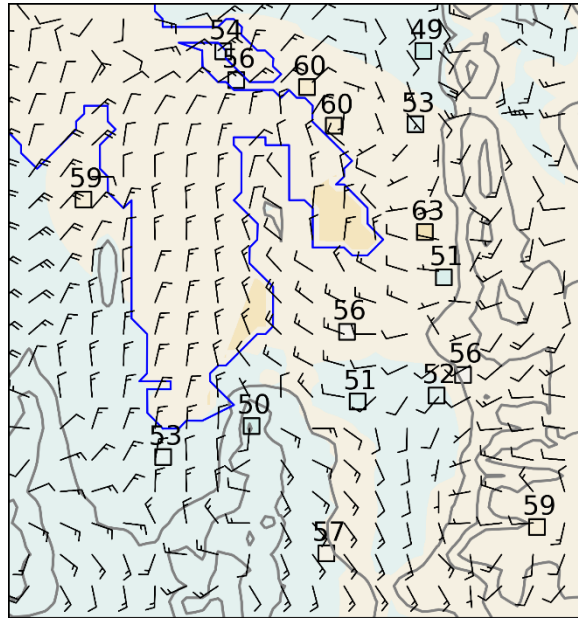
21- 23 MDT
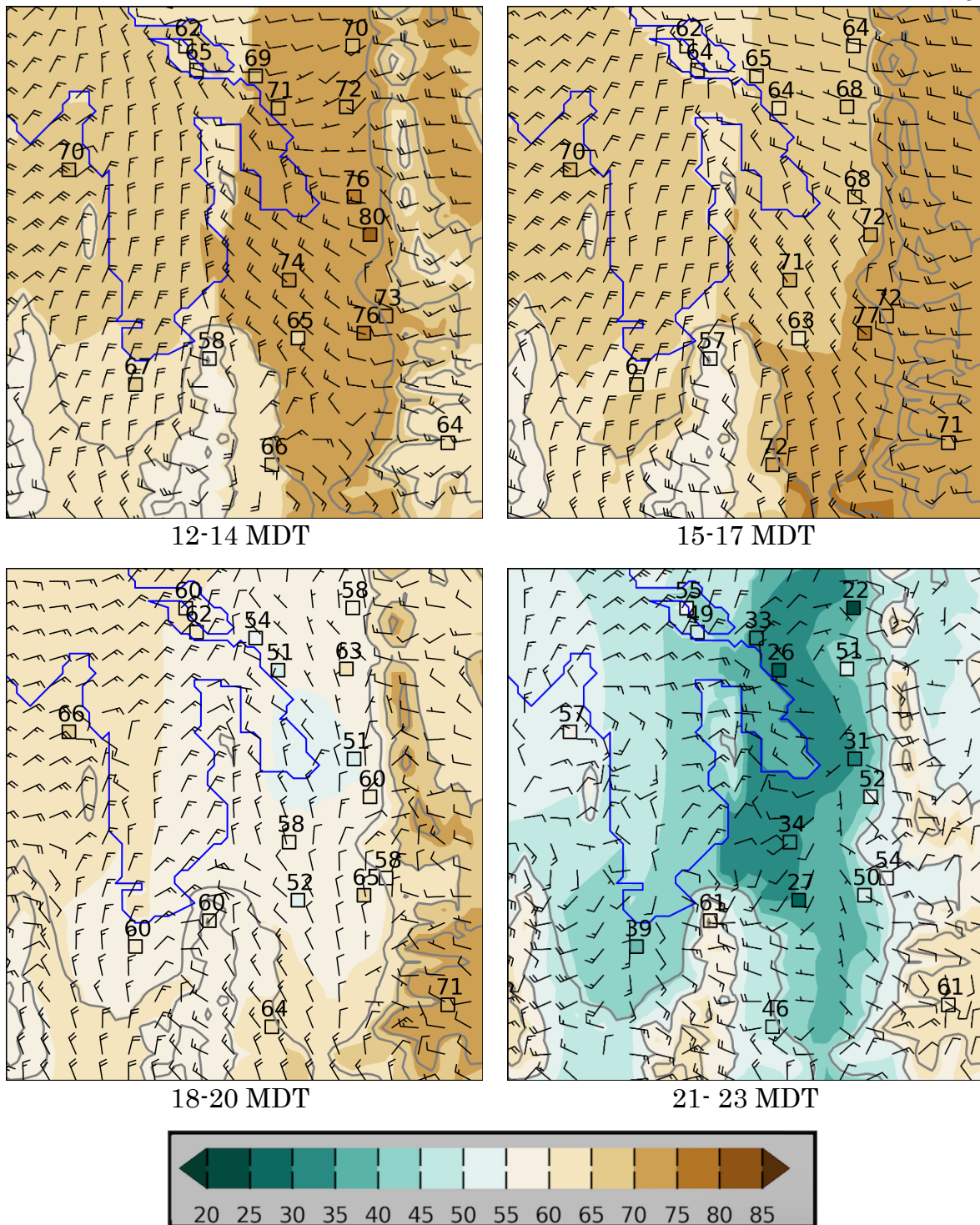
Figure 3.10. Composite ozone concentration analyses averaged over 3-hr blocks during the period 16-30 June 2015 shaded according to the colorbar. Composite vector wind analyses at every 4th gridpoint superimposed where half and full barbs denote speeds of 1.0 and 1.0 m s^{-1}. Averaged ozone concentrations during

those periods are indicated at fixed sites (squares). Elevation contoured in light grey at 500 m intervals beginning at 1500 m.

CHAPTER 4

CONCLUSION AND DISCUSSION

GSLSO3S was ~~the most~~ extensive field study conducted to investigate the processes that lead to high summer ozone concentrations over the Great Salt Lake and in urban and rural areas along the Wasatch Front. A unique dataset from mobile observations (University of Utah trucks, TRAX rail cars, and KSL5 helicopter) taken across the Salt Lake Valley and near the lake were utilized for UU2DVAR analysis to understand the spatial and temporal variability of ozone distribution and concentrations as a function of time of day. The mobile data acquired proved to be valuable in understanding how ozone ~~has distributed itself~~ across the area through UU2DVAR analyses of 18 June and 27 June 2015. KSL5 News helicopter observations were crucial in the analyses of ozone in complex terrain that surrounds the Great Salt Lake. Ozone data at GPS locations were used to effectively interpolate grid points between higher elevation stations such as Farnsworth Peak (FWP) and Snowbird (S2OZN).

The strong synoptic ridging that persisted through the last half of June 2015 provided quiescent atmospheric conditions with sparse cloud cover and

warm temperatures. No wildfires were in the vicinity so no smoke had been advected over the Great Salt Lake. From 16-30 June, at least one of the eight rural (lakeshore) stations exceeded the new NAAQS standard 70 ppb or greater, thirteen out of the fifteen days. Out of the eleven urban sites, at least one reported an 8-hr average ozone concentration of 70ppb or greater fourteen out of the fifteen days.

Using the assumptions following Tyndall and Horel (2013), the University of Utah's two-dimensional variational data analysis system was further manipulated in order to result in what is to be understood as a more representative analysis of ozone concentrations over the GSL and surrounding Wasatch Front. All meteorological background fields were generated from HRRR forecast grids while ozone background fields were linearly interpolated every hour based off of elevation and the treatment their respective categories found in Table 2.2 recieve in the analyses. Decorrelation length scales in the horizontal and vertical were also adjusted in a sensitivity test, showing that these adjustments make only minor changes in the representation of the spatial extent of ozone concentrations. Ozone concentrations across the lake were generated by bogusing 5 lakeshore stations (stations in red in Table 2.2.). Though this method created a spatial analysis of ozone concentrations over the lake effectively, the lake is sparse with data. However, by bogusing some lakeshore stations over the lake, the analysis provided a spatial analysis of ozone concentrations over the lake. The analysis of ozone concentrations in the

boundary layer over the lake can only become more delineated through the addition of more ozone monitoring stations across the lake. Helicopter flights were able to provide data in the vertical coordinate during some periods throughout the summer. This helicopter data proved to be useful to UU2DVAR analyses, as well as other mobile data from trucks and TRAX lines. The usefulness of mobile data is shown in Fig. 2.3.c. where it is evident that the UU2DVAR analyses without mobile observations is inferior to the analyses with mobile observations.

The data analyzed during this time revealed the effects on ozone concentrations by primarily local scale flows. Thermal flows such as up/downvalley, up/downslope, and canyon winds as well as with lake breezes are a function of time of day as a result of insolation changes throughout the day. Though the rise and fall of ozone levels are naturally driven by available insolation, the differential heating across the valley and GSL that occurs throughout the day results in a complex interaction of flows that have an influence on where and when ozone is distributed throughout the region. Valley flows shift ozone north and south while slope and canyon flows transport ozone and precursors in the vertical to higher elevations. The upslope winds result in high elevation stations reporting higher ozone concentrations at night than those stations within the valley. All artifacts of these processes can be seen in both 18 and 27 June case studies. One artifact in the wind analyses to note is the strong easterly flow across the lake at night. Ozone wind

roses at both Lakeside (O3S06) and Badger Island (BGRUT) stations show that winds from this direction are polluted likely as a result of a mountain/plane circulation that advects ozone polluted air from higher elevations and urban areas to the lake boundary layer.

The lake-breeze is initiated by differential heating between the land and the large body of water, and has been seen in this study to play a large role on ozone transportation across boundary layer interface between urban areas and the lake. The ozone wind roses in Fig. 3.5 show that during the day, almost all stations have a high percentage of wind coming from the direction of the lake that also coincides with high ozone values. At night, most stations have wind directions towards the lake, thus replacing the high ozone that was advected into the valley with clean air and is transported back into the boundary layer of the lake. However, at night near the mouths of some canyons and at high elevation stations show higher ozone concentrations than those on the valley floor. Ozone wind roses also show the transport of ozone via upslope winds during the late afternoon and nighttime hours from urban areas below as well as from areas downwind in the free atmosphere. The stations near the canyon mouths at night begin to receive the ozone that had been transported aloft in upslope flows when the wind direction changes at dawn to downslope flow.

This study confirms a characteristic diurnal cycle of low ozone levels at night and during the early morning hours with ozone concentrations peaking in the late afternoon amongst all categories. Urban areas also experienced

lower ozone concentrations relative to rural, lakeshore, and high elevation areas due to urban titration. Advection of ozone and ozone precursors from the valley and within the reservoir of ozone over the lake occurs primarily through and a complex interaction of slope and valley flows as well as other thermally driven circulations. Thus, the fluctuations in ozone concentration as a function of time of day in high elevation and rural (particularly along the western shore of the GSL) stations are largely dependent upon these circulations initiated by differential heating. Combined with less exposure to nocturnal urban titration, there is less of a dramatic swing in daily ozone concentrations in rural and lakeshore stations, resulting in higher concentrations at night than those in urban locations. Urban sites within the valley typically reach 0 ppb overnight due to nighttime titration and transportation of ozone into the mountains and over the lake through upslope flows and lake breezes. This information about characteristic ozone concentration patterns in rural, lakeside, and urban areas as a function of time of day help to delineate and pinpoint where and when ozone concentrations exceeded current EPA standards during the summer.

UU2DVAR ozone analyses from this study can further be of use to air quality forecasters as analyses provide a greater understanding of the transportation of ozone through complex interactions between slope, valley, canyon, and lake circulations. Parameters within the UU2DVAR, such as decorrelation length scales, were assessed through a series of sensitivity tests to determine the most representative analysis of ozone distribution across our

domain. Weightings on mobile observations from trucks and the helicopter were also tested (not shown) to determine the best spatial analysis. Using the parameters and weightings found to be the most fit for ozone analysis in the UU2DVAR system, forecasters will be able to see all of the complex circulations within the boundary layer at play and how they transport ozone throughout the region. Accuracy of local forecasts should improve based on these findings.

Further research using the dataset acquired in GSLSO3S will be used in future studies to understand air chemistry as well as biogenic and other anthropogenic factors that contribute to high concentrations of ozone during the summer. More research on boundary layer circulation impacts on ozone concentration are being conducted. Other factors such as above average precipitation totals in the spring resulting in potential biogenic consequences, shallow thermocline and low water levels in the GSL resulting in a shallower boundary layer of the GSL, and enhanced photochemical production from the increased albedo of salt flats that are located on the west side of the lake should be considered for future research.

References

Agel L., Lopez V., Barlow M., Colby F., 2011: Regional and large scale influences on summer ozone levels in Southern California. *J. Appl. Meteor. Climatol.*, **50**, 800-805, doi:10.1175/2010JAM2605.1.

Ainslie B. and Steyn D.G., 2007: Spatiotemporal trends in episodic ozone pollution in the Lower Fraser Valley, British Columbia, in relation to mesoscale atmospheric circulation patterns and emissions. J. Appl. Meteor. Climatol., **46**, 1631–1644, doi: 10.1175/JAM2457.1

Arens, S. and Harper K., 2012: 2011 Washington County Ozone Saturation Study. Accessed 13 April 2016. [Available online at http://citizensfordixie.org/wp-content/uploads/2011/11/ozone-study.pdf]

Arens S. and Harper K., 2013: 2012 Utah Ozone Study. Accessed 13   April 2016. [Available online at http://www.deq.utah.gov/Pollutants/O/ozone/docs/2013/05May/2012_Utah_Ozone_Study.pdf]

Chen T.M., Gokhale J., Shofer S., Kuschner W.G., 2007: Outdoor air pollution: ozone health effects. *Am. J. Med. Sci.*, **333,** 244-248, doi: 1097/MAJ.0b013e13803b8e8c

Cleary P. A., and Coauthors, 2015: Ozone distributions over southern Lake Michigan: comparisons between ferry-based observations, shoreline-based DOAS observations and model forecasts." *Atmos. Chem. and Phys.* **15.9**, 5109-5122, doi:10.5194/acp-15-5109-2015

Crosman E. and Horel J.D., 2016: Winter lake breezes near the Great Salt Lake, *Boundary Layer Meteor.*, **159**, 439-464, doi: 10.1007/s10546-015-0117-6

Croes B.E. and Fujita E.M., 2003: Overview of the 1997 southern California ozone study (SCOS97-NARSTO). *Atmospheric Environment,t* **37**, 3-26, doi: 10.1016/S1352-2310(03)00379-0

Doran J.C. and Zhong S., 2000: Thermally Driven Gap Winds into the Mexico City Basin. *J. Atmos. Sci.,* **39**, 1330-1340, doi: 10.1175/1520-0540(2000)039<1330:TDGWIT>2.0.CO;2

Dye T.S., Roberts P.T., Korc M.E., 1995: Observations of transport processes for ozone and ozone precursors during the 1991 Lake Michigan Ozone Study. *J. Appl. Meteor. Climatol.,* **34.8**, 1877-1889.

Environmental Protection Agency (EPA), 2015: 2015 Revision to 2008 Ozone National Ambient Air Quality Standards (NAAQS) Supporting Documents. Accessed 13 April 2016. [Available online at https://www.epa.gov/ozone-pollution/2015-revision-2008-ozone-national-ambient-air-quality-standards-naaqs-supporting]

Fast J. D. and Heilman W.E., 2003: The effect of lake temperatures and emissions on ozone exposure in the western Great Lakes region *J. Appl. Meteor. Climatol.,* **42.9,** 1197-1217.

Finlayson-Pitts B. J. and Pitts Jr. J.N., 1993: Atmospheric chemistry of tropospheric ozone formation: scientific and regulatory implications. *Air & Waste,* **43.8,** 1091-110, doi: 10.1080/1073161X.1993.10467187

Gheusi, F. and Coauthors, 2011: "Pic 2005, a field campaign to investigate low-tropospheric ozone variability in the Pyrenees." *Atmospheric Research* 101.3 (2011): 640-665, doi: 10.1016/j.atmosres.2011.04.014

Harris L. and Kotamarthi V.R., 2005: The characteristics of the Chicago Lake breeze and its effects on trace particle transport: results from an episodic event simulation. *J. Appl. Meteor. Climatol.,* **44.11**, 1637-1654, doi: 10.1175/JAM2301.1

Hastie D.R., and Coauthors, 1999: Observational Evidence for the Impact of the Lake Breeze Circulation on Ozone Concentrations in Southern Ontario. *Atmospheric Environment*, **33**, 323-325.

Horel J. and Coauthors, 2002: MesoWest: Cooperative MesoNets in the Western United States. *Bull. Amer. Meteor. Soc.*, **83.2**, 211-225, doi: 10.1175/1520-0477(2002)083<0211:MCMITW>2.3.CO;2

Horel, J. and Coauthors, 2016: Summer Ozone Concentrations in the Vicinity of the Great Salt Lake. *Atmos. Sci. Letters*, ***volume and page numbers???

Kalnay, E., 2003: *Atmospheric Modeling, Data Assimilation and Predictability*. Cambridge University Press.

Langford A.O. and Coauthors 2014: An Overview of the 2013 Las Vegas Ozone Study (LVOS): Impact of stratospheric intrusions and long-range transport on surface air quality. *Atmospheric Environment,* **109,** 305-322, doi: 10.1016/j.atmosenv.2014.08.040

Lasry F., Coll I., Buisson E., 2005: An insight into the formation of severe ozone episodes: modeling the 21/03/01 event in the ESCOMPTE region. *Atmospheric research* **74.1**, 191-215, doi 10.1016/j.atmosres.2004.04.004

Levy I., Makar P.A., Sills D., Hayden K.L., Mihele C., Narayan J., Moran M.D., Sjostedt S., Brook J., 2010: Unraveling the complex local-scale flows influencing ozone patterns in the southern Great Lakes of North America. *Atmospheric Chemistry and Physics,* **10.22**, 10895-10915, doi:10.5194/acp-10-10895-2010

Lin C.-H., Wu Y.-L., Lai C.-H., 2010: Ozone reservoir layers in a coastal environment–a case study in southern Taiwan. *Atmospheric Chemistry and Physics* **10.9**, 4439-4452, doi:10.5194/acp-10-4439-2010.

Lyons W.A. and Olssoon L.E., 1973: Detailed Mesometeorological Studies of Air Pollution Dispersion in the Chicago Lake Breeze. *J. Atmos. Sci.,* 202, 387**-403, doi: 10.1175/1520-0493(1973)101<0387.DMSOAP>2.3.CO;2**

Madronich S., Shao M., Wilson S.R., Solomon K.R., Longstreth J.D., Tang X.Y., 2015: Changes in air quality and tropospheric composition due to depletion of stratospheric ozone and interactions with changing climate: Implications for human and environmental health, *Photochem. Photobiol. Sci.,* **14**, 149-160, doi:10.1039/C4PP90037E

Ryerson T.B., and Coauthors 2013: The 2010 California Research at the Nexus of Air Quality and Climate Change (CalNex) field study. *J. Geophys. Res. Atmos.,* **118**, 5830–5866, doi: 10.1002/jgrd.50331

SCAQMD, 1997: The Southland's War on Smog: Fifty Years of Progress Toward Clean Air (through May 1997). Accessed 13 April 2016. [Available online at http://www.aqmd.gov/home/library/public-information/publications/50-years-of-progress#]

Simon H., Reff A., Wells B., Xing J., Frank N., 2015: Ozone trends across the United States over a period of decreasing NOx and VOC emissions. *Environmental Science & technology* **49.1,** 186-195, doi: 10.1021/es504514z

Tyndall, D., and J. Horel, 2013: Impacts of mesonet observations on meteorological surface analyses. *Wea. Forecasting.* **28**, 254-269, doi: 10.1175/WAF-D-12-00027.1

Whaley C.H and Coauthors, 2015: Toronto area ozone: Long-term measurements and modeled sources of poor air quality events. *Journal of Geophysical Research: Atmospheres,* **120, 11368-11390, doi: 10.1002/2014JD022984**

Zeller K.F, Evans R.B, Fitzsimmons C.K, Siple G.W., 1977:Mesoscale analysis of ozone measurements in the Boston Envi- Mesoscale analysis of ozone measurements in the Boston Environs. Journal of Geophysical Research 82(37): 5879-5888.

Zhang R., Lei W., Tie X., Hess P., 2004: Industrial emissions cause extreme urban ozone diurnal variability." *Proceedings of the National Academy of Sciences of the United States of America* **101.17,** 6346-6350, doi:10.073/pnas.0401484101